Environmental Science and Pollution Research (2021) 28:60857–60880
https://doi.org/10.1007/s11356-021-14678-9

RESEARCH ARTICLE

Trace elements in the shoreline and seabed sediments of the southern Caspian Sea: investigation of contamination level, distribution, ecological and human health risks, and elemental partition coefficient

Mohammad Javad Nematollahi[1,2,3] · Behnam Keshavarzi[1,4] · Farid Moore[1,4] · Rolf David Vogt[2,3] · Hassan Nasrollahzadeh Saravi[5]

Received: 4 March 2021 / Accepted: 28 May 2021 / Published online: 24 June 2021

Abstract

This study assesses the occurrence of trace elements (TEs) in sediments of the southern Caspian Sea. A total of 16 shoreline sediment samples and 15 seabed sediment samples along five coastal transects were studied. The mean concentration of TEs follows the order of Zn > V > Cr > Ni > Cu > Pb > Co > As > Sb > Mo > Cd. The TEs had an uneven, heterogeneous distribution within the shoreline and seabed sampling sites. This is due to that the study area comprises a large number of different pollution sources, also different sediment physicochemical characteristics. Levels of individual TEs within the seabed sediment transects were higher where their shoreline sites had higher concentrations, reflecting that the coastal sites play an important role in diffusing the contaminants towards the sea. The main anthropogenic source of TEs in this highly populated region, especially in the western part, is likely a large number of discharge points of greywater entering the sea. In addition, dominant fishing industry, tourism, intense agriculture, and textile and paper industry, as well as several other commercial activities, contribute significantly to the overall loading of TEs. Based on the statistical analyses, the organic matter and mud fraction had a strong explanatory value for the spatial variation of Cu, while oxyhydroxides of Fe and Mn had good explanatory factors to govern the spatial variation of other TEs. Pb and Zn had a relatively high partition coefficient (Kd), reflecting the affinity of these elements to be sorbed to the sediment phase. Cd and Sb had lower Kd, tending to remain in the aqueous phase. Geochemical indices indicated high enrichment of Cd, Sb, Zn, and Pb at a number of sampling sites, reflecting potential local sources of contamination. The Sisangan recreational area was identified as the most contaminated site. From a public health perspective, the non-carcinogenic risk of TEs was significant only at this site. The carcinogenic risks of Pb(II) and As(III) in adults, and Pb(II), Cd(II), and As(III) in children, were tolerable.

Keywords Distribution · Risk assessment · Trace element · Origin · Partition coefficient · SQG · Sediment · XRD

Responsible Editor: V. V.S.S. Sarma

✉ Behnam Keshavarzi
bkeshavarzi@shirazu.ac.ir

Mohammad Javad Nematollahi
m.nematollahi@shirazu.ac.ir; mjnematollahi.shirazu@gmail.com

[1] Department of Earth Sciences, College of Sciences, Shiraz University, Shiraz 71454, Iran

[2] Department of Chemistry, Faculty of Mathematics and Natural Sciences, University of Oslo (UiO), 0315 Oslo, Norway

[3] Centre for Biogeochemistry in the Anthropocene, University of Oslo, 0315 Oslo, Norway

[4] Medical Geology Center of Shiraz University, Shiraz 71454, Iran

[5] Caspian Sea Ecology Research Center (CSERC), Iranian Fisheries Science Research Institute (IFSRI), Agricultural Research, Education and Extension Organization (AREEO), Sari, Iran

Introduction

Increased population growth and consumption rate, accompanied by the rapid development of industrial activities, have contributed to the release of a huge amount of harmful pollutants into the environmental systems, inflicting severe adverse impacts especially on the coastal ecosystems reducing their environmental quality (Ribeiro et al. 2018; Nematollahi et al. 2020a). This has dire consequences as coastal and marine environments are considered among the most productive environmental systems for an extensive range of biota.

Sediment is an important compartment of the aquatic ecosystems as it serves as a net sink of pollutants. However, changes in physical and chemical factors may lead to their re-release into the water column. Contaminated sediments can thereby act as a secondary source of pollutants to the environment. Pollutants that accumulate in shoreline and seabed sediments induce adverse effects on its living organisms, imposing a fast degradation of coastal and marine ecosystems (Ruiz-Compean et al. 2017). Since sediments store pollutants, they are generally used to locate pollutant hotspots, identify dispersion routes, and thereby determine the origin of pollutants in coastal and marine systems (Ruiz-Compean et al. 2017). Furthermore, compared to the dynamic overlying water column, the levels of contaminants in the sediment provide a static measure to evaluate the state of the environment in regards to the anthropogenic pressures, and the risk caused by the pollutants in the aquatic environments. Synoptic environmental surveys of the levels of contaminants in sediments are therefore commonly conducted to gain good insight into the state-of-the-environment in coastal and marine ecosystems.

Trace elements (TEs), in biochemistry commonly referred to as heavy metals comprising type B (soft) and some intermediate elements, are ubiquitous pollutants in coastal and marine ecosystems causing detrimental effects to aquatic biota. These elements represent an environmental concern because of their numerous anthropogenic sources, long residence time in the environment, easy bioaccumulation in aquatic biota, and toxic effects (Moore et al. 2015, Rosado et al. 2016, Duan et al. 2018, Bing et al. 2019). Due to their low solubility, the TEs in aquatic systems are mainly found adsorbed to suspended particles and thus in the sediments (Merhaby et al. 2018, Bing et al. 2019). Sediments are, therefore, especially suitable to monitor the contamination of TEs.

Many studies have assessed the levels of TEs in coastal and marine sediments (e.g., Delshab et al. 2017, Liu et al., 2018, Zhao et al., 2018, Xu et al., 2018, El Baz and Khalil, 2018, Li et al. 2019, Tunde et al. 2020). There also exist a few such studies conducted along the Mazandaran province coasts in the southern Caspian Sea (Tabari et al. 2010, Agah et al. 2011, Naji and Sohrabi 2015, Alizadeh et al. 2018, Mirnategh et al. 2018, Abadi et al. 2019). Though, to the best of our knowledge, this is the first assessment of the levels of TEs in both shoreline and seabed sediments of the Mazandaran province coasts in the southern Caspian Sea. The present study maps the spatial distribution and concentrations of TEs within shoreline and seabed sediments of the Caspian Sea coastal zone of the Mazandaran province, Iran, evaluating their impact on ecological and human health.

Study area

General properties and location of the study area

The Caspian Sea is the world's largest inland water body and surrounded by the littoral countries of Iran, Russia, Azerbaijan, Turkmenistan, and Kazakhstan. It has a surface area of 396,000 km^2, a length of 1200 km, and a mean width of 330 km, with a mean depth of 201 m. As the lake is endorheic, the water in the south has a mean salinity of 12-13 ppt and a pH of 8.5 (Nematollahi et al. 2020a). The southern Caspian Sea coasts stretch about 920 km through the Iranian subtropical Mazandaran, Guilan, and Golestan provinces, of which the coastal length of Mazandaran province comprises 487 km. About 130 rivers flow into the Caspian seawater, discharging annually about 300 km^3 of water. The largest river is the Volga, Europe's longest river, entering into the Caspian Sea from the north (CEP 2002). Iranian rivers contribute about 5% of the total recharge (Alizadeh et al. 2018). Sediment delivery to the Iranian coastal zones of the southern Caspian Sea is mainly provided by 61 rivers (Afshin 1994). Traditionally, agriculture, fishery, and tourism have been among the most important commercial practices in the study area, though the number of industrial activities has grown exponentially since 1960 (Alizadeh et al. 2018) in this densely populated region.

The study area is the coast of Mazandaran province (Fig. 1) in Iran, which holds the longest shoreline in the southern Caspian Sea. Water currency along the coast flows from west to east (Bohluly et al. 2018). Two main rivers to the west of the area, Kura in the south of the Azerbaijan Republic and Sefidrud in Iran, are major sources of contaminants to the water and coastal sediments of the southern Caspian Sea (Voropaev et al. 1986, Nematollahi et al. 2020a). In addition, there are 61 Iranian rivers and local streams (e.g., Tajan, Chalus, Babolrud, Nekarud, Sardabrud, Tonekabon, and Haraz) as well as numerous point outlets from local wastewater and surface runoff that emit contaminants to the sea.

Geologic setting of the study area

Mazandaran province comprises a variety of geological formations (see Supplementary Material 1), ranging in age from Precambrian slaty shales with sandstone to the recent alluvium deposits including low-level pediment fan and valley terrace

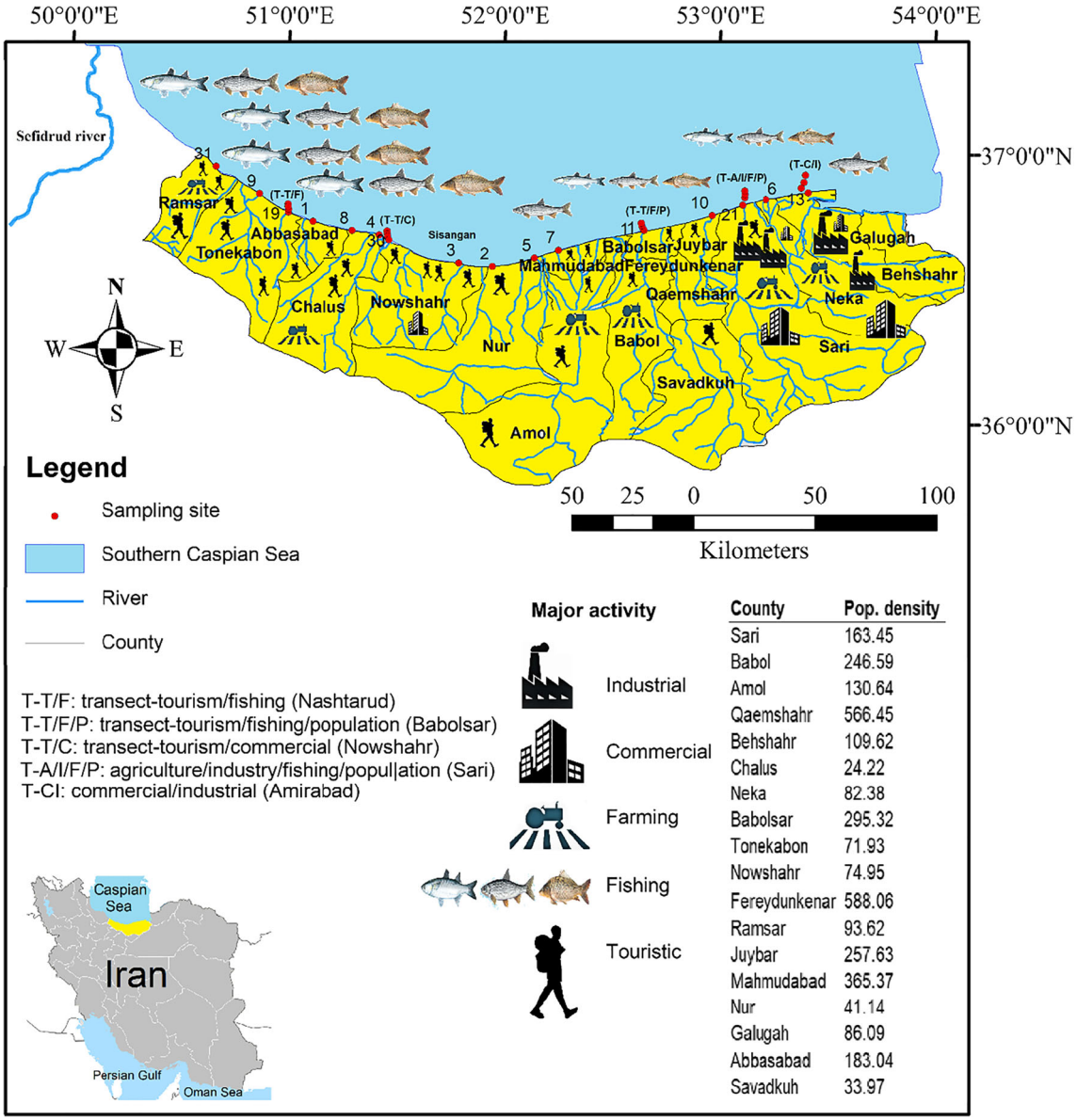

Fig. 1 A schematic map illustrating the study area, position of sediment sampling sites (#1-31), and the dominant anthropogenic activities or major sources of elements in the area

deposits. The study area includes igneous and sedimentary rocks on top of the Precambrian basement. The main lithologies consist of limestone, dolomite and shaly limestone, shale and sandstone, and conglomerate, as well as some basaltic volcanic rocks. The volcanic rocks are mainly located in the far southern reaches of the province, while the carbonaceous sedimentary rocks are situated in the vicinity of the sea and play a significant role in controlling the mineralogical composition of the Caspian Sea sediments.

Particles have been transported from land to the Caspian Sea through fluvial and eolian processes (Lahijani and Tavakoli 2012), the eruption of mud volcano (Evans et al. 2007), and biogenic activities (Klige and Selivanov 1995, Giralt et al. 2003). In the sea, climate, sea currents, and bottom topography mainly govern the distribution pattern of sediments (Kostianoy and Kosarev 2005).

Materials and methods

Sampling and sample preparation

Sediments were collected from 16 shoreline and 15 seabed sites during the dry season in May 2019. At each site, about 1 kg of composite sediment sample, comprising a mixture of 5 subsamples, was collected. The shoreline sediment samples were collected using a stainless-steel shovel. Seabed sediments were taken along five coastal transects using a Van

Veen grab sampler. More specific information on each sampling site is given in Supplementary Material 2. Seabed sediment samples were collected along five coastal transects where the water depths were 5, 10, and 20 m. Site selection for each transect was based on that at least a dominant source of TEs is pervasive. Therefore, each transect reflects the influence of either tourism/fishing/population (T/F/P: Babolsar), tourism/commercial (T/C: Nowshahr), tourism/fishing (T/F: Nashtarud), agriculture/industry/fishing/population (A/I/F/P: Sari), and commercial/industry (C/I: Amirabad). Collected sediment samples were transported in plastic bags. The location and major features of each sediment sampling site are described in Supplementary Material 2.

Sample treatment and analysis

The collected sediment samples were treated at the lab of the Shiraz University Medical Geology Center. Sediment samples were first spread on plastic plates and left to dry out at room temperature. Samples for pH, conductivity (EC), and texture determination were passed through a standard 2-mm sieve. Samples for elemental analysis of the silt and clay fraction (mud) were passed through a 63-μm sieve before 2 g of each sample was stored in clean plastic bags, and transported to the Zarazma Mineral Studies Company (Iran) for elemental analysis. Levels of major and trace elements in the sediments were identified using inductively coupled plasma-optical emission spectrometry (ICP-OES, Agilent model 7500, Agilent, USA) after Aqua Regia Digestion.

Electrical conductivity (EC) and pH of sediment samples were measured according to methods presented by Ryan et al. (2007) and Pansu and Gautheyrou (2007). A total of 25 g of dried and sieved sediment sample was mixed with 62.5 mL of deionized water, mixed for about 5 min. The supernatants were then passed through an S&S Whatman paper, before pH and EC of the filtrate were measured using a pH/EC meter (Eutech instrument, Waterproof CyberScan, PCD 650, Singapore). Organic matter (OM) and inorganic carbonate (CO_3^{2-}) were measured by the loss on ignition at 550°C and 950°C, respectively (Heiri et al., 2001), using a high-temperature furnace (Carbolite company, Sheffield, UK). The texture of samples, including the percentage of clay, silt, and sand, was determined using the hydrometry method (Bouyoucos 1962). To determine the effective cation exchange capacity (CEC) of sediment samples, the USEPA test method 9081 A was applied (USEPA 1986; Ryan et al. 2007).

The crystalline mineralogical composition of sediment samples was identified at the University of Oslo, Norway, using routine powder X-ray diffraction (XRD) (RECX-DIFF-5, D8 Discover), applying continuous radiation and step sizes of 0.02° from 10 to 70° 2 .

Quality control

Before conducting laboratory operations, the benches were cleaned using ethanol. All laboratory glassware and equipment were treated in compliance with the standard cleaning protocols described by Moore et al. (2015). Lab glassware and tools were washed using phosphate-free soap and rinsed with deionized type II water and left semiclosed at room temperature to dry out. For each parameter, all samples were analyzed by the same operator. Solutions and reagents used in this study were of the standard Merck grade. Quality control and assurance of the data obtained from the analysis were checked using blind and blank samples, replicate spectroscopic measurements for four samples, and analysis of certified reference materials (CRM). Overall, four duplicate samples were analyzed to confirm the precision of the analytical instrument and thus the results of the analytical data. Blank samples and CRMs (Oreas 902, 903, 905, and Geostats 308-12, 903-13, 907-13) were applied to ensure the accuracy of the analytical instruments and the detection limit. In every batch of the sediment samples for analysis, two blank samples were prepared and analyzed. The concentrations of all blank samples were below the detection limit of the instrument. The recovery percentages of the analyzed samples ranged from 90 to 110 %. All the analytical results were satisfactory and confirmed the precision and accuracy of the instruments.

Data analysis

Spatial distribution of sampling points and analytical data were assessed using Arc-GIS version 10.3. SPSS version 22 was applied to do statistical tests. The statistical Shapiro-Wilk (S-W) test was used to check data normality. Spearman correlation coefficients were applied to determine possible significant empirical relationships between elements and physicochemical parameters of shoreline and seabed sediments.

Source apportionment of elements was attempted to be assessed by cluster analysis (CA) and principal component analysis (PCA) using Minitab 18. To run the CA model, the complete linkage method and the correlation coefficient distance measurement were applied. The PCA model was run based on the eigenvalues greater than one and the varimax rotation technique (Nematollahi et al. 2020b). Before running the PCA, the data was normalized using the Kaiser normalization method to achieve the optimum quantity of components. Kaiser–Meyer–Olkin technique was applied to estimate the sampling adequacy (Nematollahi et al. 2020c).

Ecological risk of TEs

Ecological risks posed by the levels of TEs in sediment samples were assessed by using several geochemical indices

described below. For each index, the qualification classes with their border values are listed in Supplementary Material 3.

Single-elemental geochemical indices Contamination factor (CF) and contamination degree (CD), suggested by Hakanson (1980), are geochemical indices commonly used to evaluate the contamination of toxic substances in sediments of aquatic media. CF reflects the contamination by an individual substance, whereas CD indicates the overall contamination regarding the sum of the estimated CFs for individual contaminants at each sampling site. The indices are computed according to Eqs. 1 and 2 (Hakanson 1980).

$$\mathrm{CF} = \frac{\mathrm{C_s}}{\mathrm{C_r}} \tag{1}$$

$$\mathrm{CD} = \sum_{\mathrm{i=1}}^{\mathrm{j=n}} \mathrm{CF^i} \tag{2}$$

where C_s and C_r are the concentrations of an individual substance in the sediment sample and the preindustrial reference level, respectively. Regarding either the CF or CD, the sediment quality is classified into four classes, as presented in Supplementary Material 3.

Enrichment factor (EF) is widely applied to evaluate the anthropogenic enrichment of substances relative to their geogenic concentrations. Here the ratios of TEs over a common conservative major geogenic element are compared to their ratios in a reference background medium, such as sediment samples or continental crust (UCC) (Duodu et al. 2016, Samanta et al. 2017). The EF was calculated using Eq. 3 (Sutherland 2000).

$$\mathrm{EF} = (\mathrm{C_s}/\mathrm{C_r})/(\mathrm{B_s}/\mathrm{B_r}) \tag{3}$$

where C_s and C_r are the content of a given TE in the sample and in the background reference medium, and B_s and B_r are the content of the conservative geogenic reference element in the sample and the reference medium, respectively. Aluminum (Al) was taken as the reference element in this study due to its normal distribution and relatively low variations within the sediment samples and upper continental crust (UCC). Al is also widely used as a normalizing element in coastal and marine sediments (Maanan et al. 2015). The degree of pollution by the TEs in the sediments was estimated based on the EF reference values presented in Supplementary Material 3 (Qingjie et al. 2008).

Multi-elemental geochemical indices Modified contamination degree (MCD), Nemerov Pollution Index (NPI), and Modified Pollution Index (MPI) are among widely used multi-elemental geochemical indices to investigate the combined impact of pollution by several substances in sediments (Brady et al. 2015). The MCD and NPI, proposed by Hakanson (1980) and Qingjie et al. (2008), respectively, are both commonly used geochemical indices for assessing the combined effect of a number of pollutants in an environment. The MPI considers the contamination of substances in an environment regarding its complicated non-conservative manner, as well as the background concentrations of the substances using the calculated EFs (Brady et al. 2015). MCD, NPI, and MPI are calculated by Eqs. 4, 5, and 6, respectively.

$$MCD = \frac{\sum_{i=1}^{j=n} CF^i}{n} \tag{4}$$

$$NPI = \sqrt{\frac{(CF_{Ave})^2 + (CF_{Max})^2}{2}} \tag{5}$$

$$MPI = \sqrt{\frac{(EF_{Ave})^2 + (EF_{Max})^2}{2}} \tag{6}$$

Ecological risk Potential Ecological Risk Index (Er), suggested by Hakanson (1980), is commonly applied to estimate the potential ecological risk related to pollution by a substance in the environment. Modified Ecological Risk Index (MRI) uses the EFs rather than the CFs in the basic formula (Brady et al. 2015). The point with MRI is that it relates the levels of TEs to the natural lithologic and terrestrial inputs of TEs to the sediments (Duodu et al. 2016). MRI is computed using Eqs. 7 and 8 (Brady et al. 2015).

$$\mathrm{Er}^i = \mathrm{Tri}^{\mathrm{i}} \times \mathrm{EFi}^{\mathrm{i}}; \tag{7}$$

$$\mathrm{MRI} = \sum_{\mathrm{i=1}}^{\mathrm{n}} \mathrm{Er}^{\mathrm{i}}, \tag{8}$$

where Tr^i is the toxic response of a given TE (i.e., zinc (Zn) = 1, chromium (Cr) = 2, copper (Cu) = lead (Pb) = nickel (Ni) = 5, arsenic (As) = 10, and cadmium (Cd) = 30). Based on Er^i and MRI values, the sediment quality is categorized into several classes as listed in Supplementary Material 3 (Hakanson, 1980).

Sediment quality

Sediment quality guidelines (SQGs) are used for benchmarking the tolerable content of TEs in sediments and thereby predicting the potential toxicity of the pollutants to the biota living in or near the sediment. The overall toxicity of contaminated sediments can thereby be assessed by relating their non-normalized and normalized (by the mud sediment content < 63 μm) measured content of TEs to those of SQG (Violintzis et al. 2009). The SQG is mainly applied in monitoring programs to rank the degree of concern regarding different contaminated areas or contaminants (Long and MacDonald 1998). SQGs comprise effects range-low/effects range-median (ERL/ERM), and threshold effects levels/probable effects levels (TEL/PEL) (Long et al. 1995).

Adverse toxic impacts of TEs in sediments are rarely the case when the SQG <ERL or <TEL, occasionally when SQR is similar to TEL/PEL or ERL/ERM, and common if SQR is >PEL or >ERM (Smith et al. 1996, Menchaca et al. 2012). Mean ERM or PEL quotients (mERMQ, mPELQ) (Eq. 9) are practical for comprising large amounts of data on several TEs and their toxic effect into a single number (McCready et al. 2006). Hence, mERMQ and mPELQ provide a more practical measure to assess toxicity than the simple compilation of ERM and PEL numbers.

$$\text{mERMQ or mPELQ} = \frac{\sum\left(\frac{C_i}{\text{ERM}_i \text{or PEL}_i}\right)}{n} \quad (9)$$

where C_i, ERM_i and PEL_i, and n are the content of an individual TE in the sediment, the guideline values for a given TE, and the number of TEs, respectively. When simply calculating mean quotients, the adverse impacts of contaminants to the aquatic organisms are assumed to be additive instead of antagonistic or synergistic. The percent probability of toxic effect for the living organisms in the sediment is determined regarding the mERMQ and mPELQ values as follows: 12 % (mERMQ < 0.1), 30 % (0.11 ≤ mERMQ ≤ 0.5), 46 % (0.51 ≤ mERMQ ≤ 1.5), 74 % (mERMQ ≥ 1.51), 10 % (mPELQ < 0.1), 25 % (0.11 ≤ mPELQ ≤ 1.5), 50 % (1.51 ≤ mPELQ ≤2.3), and 76 % (mPELQ ≥ 2.3). Based on the derived percent toxicity, the sediment sites are qualitatively categorized into four classes of low, low to medium, medium to high, and high priority sites (Long and MacDonald 1998).

Partition coefficient of TEs

Distribution of TEs in aquatic media is governed by their partitioning between the solid and aqueous phases (Turner 1996, Singovszka et al. 2017, Feng et al. 2017, Thanh-Nho et al. 2018). The partition coefficient (Kd) of elements is calculated using Eq. 10.

$$K_d = \frac{C_s}{C_d} \quad (10)$$

where Kd is in L kg^{-1}, C_s and C_d are the concentrations of a given TE in the solid phase (sediment) in mg kg^{-1}, and in dissolved phase (water) in mg L^{-1}, respectively. Partition coefficient provides a good insight into the combined effect of desorption and adsorption processes of TEs. It is also important in the hydrogeochemical modeling and assessment of contamination effects. In this study, concentrations of TEs in water samples (C_d), collected from the same stations as the shoreline sediment samples, were extracted from Nematollahi (2020).

Human health risk of TEs

The human exposure and health risk of TE in sediment samples were computed using the USEPA (2011) method. In this method, non-carcinogenic and carcinogenic risks are introduced as the Hazard Index (HI) and the incremental lifetime cancer risk (ILCR), respectively, and are computed using Eqs. 11-17 (USEPA 2011).

$$\text{ADD}_{\text{ing}} = C_S \times \frac{\text{IngR} \times \text{EF} \times \text{ED} \times \text{CF}}{\text{BW} \times \text{AT}} \quad (11)$$

$$\text{ADD}_{\text{inh}} = C_S \times \frac{\text{InhR} \times \text{EF} \times \text{ED}}{\text{BW} \times \text{AT} \times \text{PEF}} \quad (12)$$

$$\text{ADD}_{\text{derm}} = C_S \times \frac{\text{AF} \times \text{EF} \times \text{SA} \times \text{ABS} \times \text{FE} \times \text{ED} \times \text{CF}}{\text{BW} \times \text{AT}} \quad (13)$$

$$\text{HQ}_i = \sum_{p=1}^{3} \frac{\text{ADD}_P}{\text{RfD}_i} \quad (14)$$

$$\text{CR}_i = \sum_{p=1}^{3} \text{ADD}_{ip} \times \text{SF}_{ip} \quad (15)$$

$$\text{HI} = \sum_{i=1}^{n} \text{HQ}_i \quad (16)$$

$$\text{ILCR} = \sum_{p=1}^{3} \text{CR}_i \quad (17)$$

where ADD is the average daily dose (mg·kg^{-1}·day^{-1}) of an individual TE through ingestion (ADD_{ing}), inhalation (ADD_{inh}), and dermal contact (ADD_{derm}), and RfD_{ip}, HQ_i, SF_{ip}, and CR_i are the reference dose, hazard quotient, slope factor, and cancer risk for a given toxic element, respectively. Detailed information on the presented formula and factors is listed in Supplementary Material 4. An HI value less than one suggests no risk, whereas a value above unity poses a potential risk (USEPA 2011). An ILCR value < 10^{-6} and > 10^{-4} reflects negligible and high risks of TEs for cancer development, respectively (USEPA 2011).

Results and discussion

Physiochemical characteristics of sediment

Main physical and chemical properties of shoreline, seabed, and all sediment samples are listed in Table 1. The pH varies between 7.83 and 8.55; hence, the sediments are slightly alkaline. This is because of the high carbonate content of the sediment, varying between 4.60 and 17.4%. Due to the high pH, TEs with high covalent index (type B or soft elements) have low solubility, except for the elements that form oxyanions (e.g., As(IV, VI) and Cr(VI)). The high carbonate content in the sediment samples mainly originates from the

Table 1 Statistical summary of the physicochemical characteristics in shoreline, seabed, and all sediment samples

Medium	St.	pH	EC (mS/cm)	OM (%)	CO3 (%)	CEC (meq/100g)	Sand (%)	Silt (%)	Clay (%)
Shoreline	Min.	8.0	0.2	0.3	4.6	3.9	78.8	0.1	0.3
(N = 16)	Max	8.6	5.1	3.3	17.4	21.4	99.5	10.6	12.9
	Mean	8.4	2.2	1.9	11.0	9.0	93.1	2.3	4.6
	Med.	8.4	2.4	2.0	10.8	6.7	96.2	1.1	3.1
	S.D.	0.1	1.5	0.6	3.2	5.6	6.5	2.9	4.6
	C.V.	58.8	1.4	3.0	3.4	1.6	14.4	0.8	1.0
	Skew.	−1.6	0.3	−0.5	0.3	1.4	−1.0	2.0	1.0
	Kurt.	3.2	−1.0	2.7	0.1	0.8	−0.2	3.8	−0.6
	S-W	0.027	0.339	0.200	0.741	0.002	0.014	0.000	0.003
Seabed	Min.	7.8	3.5	2.8	7.0	6.5	8.1	5.3	0.6
(N = 15)	Max	8.3	17.3	8.4	12.4	72.7	93.2	68.6	54.3
	Mean	8.1	8.6	5.4	9.5	29.2	42.4	30.1	27.5
	Med.	8.1	8.7	5.6	9.4	25.8	36.4	37.6	26.3
	S.D.	0.2	3.9	1.9	1.8	18.1	29.1	19.1	15.5
	C.V.	50.5	2.2	2.8	5.4	1.6	1.5	1.6	1.8
	Skew.	0.2	0.6	0.1	0.2	0.9	0.4	0.2	0.1
	Kurt.	−0.9	0.0	−1.3	−1.2	0.9	−1.2	−0.7	−0.8
	S-W	0.574	0.525	0.294	0.474	0.303	0.210	0.175	0.755
All	Min.	7.8	0.2	0.3	4.6	3.9	8.1	0.1	0.3
(N = 31)	Max	8.6	17.3	8.4	17.4	72.7	99.5	68.6	54.3
	Mean	8.2	5.3	3.6	10.3	18.8	68.6	15.7	15.7
	Med.	8.3	4.1	2.8	9.9	11.1	83.8	6.2	10.6
	S.D.	0.2	4.3	2.2	2.7	16.5	32.9	19.3	16.1
	C.V.	39.9	1.2	1.6	3.8	1.1	2.1	0.8	1.0
	Skew.	−0.3	1.0	0.8	0.7	1.6	−0.8	1.2	1.0
	Kurt.	−1.1	0.5	−0.5	0.9	2.5	−0.9	0.3	−0.1
	S-W	0.113	0.006	0.002	0.466	0.000	0.000	0.000	0.000

EC electric conductivity, *OM* organic matter, *CEC* effective cation exchange capacity, *SD* standard deviation, *CV* coefficient of variation, *Skew* skewness, *Kurt* kurtosis, *S-W* Shapiro-Wilk test

weathering of the predominant sedimentary bedrock, including limestone, in the Mazandaran watersheds. The EC in the sediments ranges from 0.24 and 17.28 mS/cm. The EC of sediment conceptually pertains to the CEC, which is governed by other physical and chemical parameters (e.g., the content of sediment OM and texture) (Barbosa and Overstreet 2011).

The OM content is low, ranging from 0.30 to 8.39%. The texture of the sediments varies considerably, with relative contents of sand, silt, and clay size fractions ranging from 8.08 to 99.5%, 0.12 to 68.6%, and 0.36 to 54.3%, respectively. The effective CECs of the sediments range from 3.9 to 72.7 meq/100g. The relatively low CEC in the sediments is mainly because of the low content of OM and clay minerals. Derived from sedimentary bedrock, the clay size fraction is composed of oxides rather than clay minerals. As shown by the triangular Shepard diagram (see Supplementary Material 5), the sand fraction dominates in the shoreline sediment samples, while the seabed sediment samples are mainly composed of the finer silt and clay fractions. The content of clay size fraction, as well as OM, facilitates the adsorption of TEs onto the sediment material. Therefore, higher concentrations of TEs are expected in the more organic-rich and finer textured seabed sediments than in the shoreline sand samples.

Empirical relationships in the spatial distribution of physicochemical characteristics of the sediments were assessed by statistical tests. The S-W test reflects a non-normal distribution of pH, CEC, sand, silt, and clay ($p < 0.05$) only in shoreline sediments. The kurtosis values, giving the extent of outliers in the distribution, fall in or close to the range of −3 to +3, reflecting normal distribution. The skewness values of the data fall inside or close to −1 to +1. As a rule of thumb, it is not needed to transform the data when the skewness values of the variables lay within the range of −1 to +1 (Nematollahi et al. 2020b). The CV value for pH is higher than for the other parameters, reflecting that it is mainly non-normally distributed within shoreline and seabed sediments.

Figure 2 illustrates the spatial distribution of the sediment physicochemical parameters. Carbonate, clay, silt, and OM have higher content in the eastern part of the region. These parameters also increase in the seabed out through the sea transect. The higher content of carbonate in the east of the study area can be due to the thick-bedded to massive limestone of the Kope Dagh Mountain (TMS is Supplementary Material 1) situated in the Gorgan river catchment area in

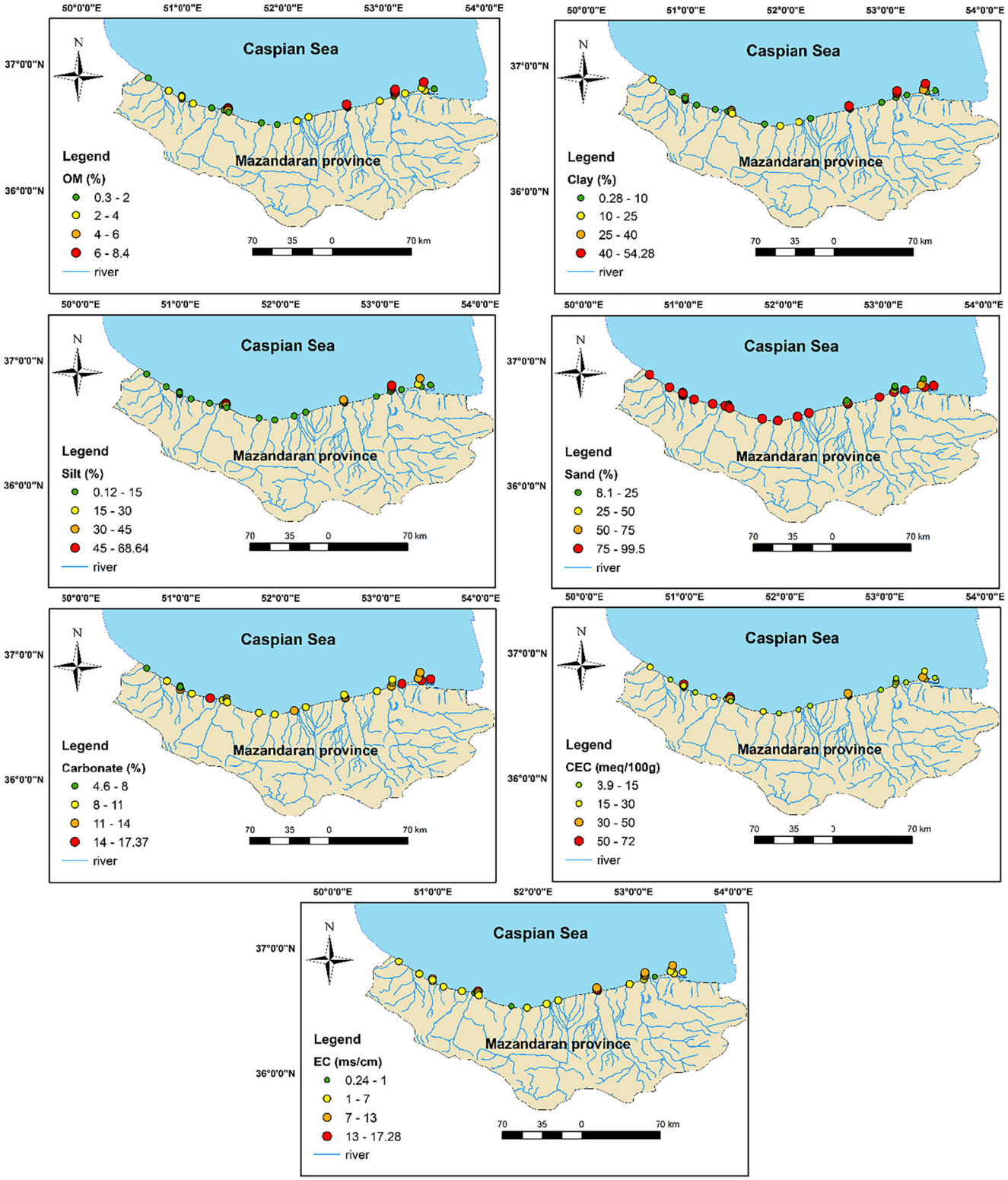

Fig. 2 Spatial distribution of the sediment physicochemical parameters

the east of Mazandaran (Lahijani and Tavakoli 2012). There is a significant correlation between CEC and mud fraction (i.e., the sum of silt and clay size fraction), reflecting higher charge density of mud fraction (Lahijani and Tavakoli 2012). There is also a significant correlation between OM content and the percentage of clay and silt in the sediment. These sediments, rich in OM and mud fraction, have a strong capacity to bind TEs.

Sediment mineralogy

Crystalline mineralogy of the sediment samples is presented in Supplementary Material 7. The samples displayed a relatively homogenous mineralogical pattern. Quartz and calcite were the dominant minerals in all samples. The small variations in the mineralogy of the samples may be due to the predominantly sedimentary bedrock of different lithology as limestone, shale, and sandstone in the region (see Supplementary Material 1). The prevalence of quartz is due to the igneous nature of silicate quartz sand, while the prevalence of sedimentary bedrock in the region causes the calcite to dominate. Based on the mineralogy, it appears clear that the sediments in the southern Caspian are mainly made up of secondary minerals originated from the nearby sedimentary bedrock. Other crystalline minerals that were observed in the sediments are clays (e.g., vermiculite), pyroxene, and oxide minerals (e.g., rutile (TiO_2) and pyrolusite (MnO_2)). The content of hydrous aluminum phyllosilicate clay minerals, such as kaolinite, illite, and chlorites, is low, due to the prevalence of carbonate bedrock. As discussed above, the clay size fraction is thus mainly composed of amorphous oxi-hydroxides and carbonate minerals. These per se have less capacity to adsorb TEs compared to clay minerals, though the large surface of the clay size fraction coated with oxyhydroxides having –OH functional groups would cause large sorption capacity. This may partly explain why the concentration of TEs in the sediments is rather low.

Distribution of TEs

The contents of major and trace elements in sediment samples and in UCC background values (Holland and Turekian 2010) are presented in Table 2. The mean contents of elements in all the studied sediments are as follows: iron (Fe) > aluminum (Al) > manganese (Mn) > Zn > vanadium (V) > Cr > Ni > Cu > Pb > cobalt (Co) > As > antimony (Sb) > molybdenum (Mo) > Cd. Based on the S-W test, the concentrations of Al, Mo, Ni, and Sb are normally distributed ($p > 0.05$), while other elements show a non-normal distribution ($p < 0.05$). Based on the skewness and kurtosis values, the contents of Al, As, Cd, Cu, Mo, Ni, and Sb are normally distributed ($-1 <$ Skew $< +1$, $-3 <$ Kurt $< +3$).

The spatial distribution of the major and trace elements based on their concentrations within the shoreline and seabed sediment samples is illustrated in Fig. 3. The highest concentrations of TEs in the shoreline sediments are found at the following locations: Cr, and Co in Sisangan (S3) and Nashtarud (S19), Zn in Sisangan (S3) and Nashtarud (S19), V and Sb in Sisangan (S3), Ni in Sisangan (S3) and Babolsar (S11), Cu in Amirabad (S13), Sari (S21), Babolsar (S11), and Nowshahr (S30), Cd in Sisangan (S3), Amirabad (S13), Sari (S21), Nowshahr (S30), and Nashtarud (S19), Pb in Sisangan (S3) and Royan (S2), As in Nowshahr (S30) and Nashtarud (S19), and Mo in Nashtarud (S19), Abbasabad (S1), Nowshahr (S30), Sisangan (S3), Mahmudabad (S7), and Larim (S10).

Overall, TEs show an uneven spatial distribution in the southern Caspian Sea sediments. This is probably due to the fact that the levels are governed both by a large number of different anthropogenic sources of pollutants and by the ability of the sediments to sorb the elements, i.e., Kd governed by texture and OM content. Main features and human activity in different sectors of the study area are shown in Fig. 1. Elevated concentrations of Ni and Pb are found in some central sites, Cu and As in some sites in the west and east, and Cr, Co, V, Sb, and Zn in some sites in the center and west of the region. The most striking feature in the spatial distribution of most TEs (except Cu and As) is their high concentrations in the Sisangan recreational area (S3). The TEs are also unevenly distributed within the sea transects. Generally, the concentration of TEs within the seabed sediment transects, where also their shoreline sites had high concentrations, was high, reflecting that the shoreline sites play an important role in diffusing TEs towards the sea. TEs in seabed sediments had higher concentrations than in shoreline sediments which could be due to the higher content of OM and mud fraction in seabed sediments relative to shore sediments (see Table 1). Moreover, the higher contents of mud size fraction and OM with increasing sea depth facilitate the greater adsorption of TEs onto the sediment material. Therefore, a higher content of TEs was found in seabed sediments from deeper water depth (i.e., 10 and 20 m).

The relative level of contamination of the study area was assessed by comparing the mean concentrations of selected TEs in the sediments with those of the other locations of the Caspian Sea and the world in the literature (Table 3). Among studies carried out in different locations of the Caspian Sea, the sites within Iran, including this study, had higher concentrations of most TEs, while the concentrations of most TEs were relatively lower in the Caspian sediments of Azerbaijan, Kazakhstan, and Russia. That the southern parts of the Caspian Sea have higher concentrations of TEs can be due to the general current of the Caspian seawater being towards the south, as well as the higher evaporation rate as reflected by the higher salinity in the south. Thus, TEs can be transported

Table 2 Statistical summary of the concentrations of TEs (in mg kg^{-1}) and major elements (in %) in shoreline, seabed, and all sediment samples

Medium	St.	Al (%)	Fe (%)	Mn (%)	As (mg/kg)	Cd (mg/kg)	Co (mg/kg)	Cr (mg/kg)	Cu (mg/kg)	Mo (mg/kg)	Ni (mg/kg)	Pb (mg/kg)	Sb (mg/kg)	V (mg/kg)	Zn (mg/kg)
Shoreline	Min.	0.6	1.7	0.0	2.1	0.2	5.0	23.0	7.0	0.5	19.0	5.0	0.7	22.0	39.0
(N = 16)	Max	1.6	10.1	0.1	7.2	0.2	30.0	576.0	53.0	0.8	57.0	61.0	0.9	738.0	270.0
	Mean	1.0	4.0	0.1	4.1	0.2	13.5	105.7	21.2	0.6	36.2	24.4	0.8	122.2	101.8
	Med.	0.9	3.9	0.1	4.1	0.2	12.5	67.0	16.5	0.6	35.5	19.5	0.8	63.5	100.0
	S.D.	0.3	1.9	0.0	1.8	0.0	5.9	130.2	13.7	0.1	9.8	16.9	0.0	170.0	50.6
	C.V.	3.3	2.1	2.8	2.3	20.8	2.3	0.8	1.5	9.2	3.7	1.4	19.6	0.7	2.0
	Skew.	0.9	2.2	1.8	0.2	−0.8	1.4	3.5	1.7	0.9	0.4	1.1	0.7	3.6	2.6
	Kurt.	0.1	7.0	5.5	−1.5	3.7	3.4	13.3	2.3	0.1	−0.1	0.7	0.5	13.5	8.8
	S-W	0.167	0.002	0.008	0.046	0.003	0.061	0.000	0.001	0.105	0.912	0.035	0.467	0.000	0.000
Seabed	Min.	1.0	2.9	0.1	2.1	0.2	11.0	50.0	16.0	0.5	38.0	14.0	0.7	40.0	86.0
(N = 15)	Max	1.9	7.2	0.1	7.3	0.2	22.0	186.0	63.0	0.7	52.0	40.0	0.8	296.0	169.0
	Mean	1.5	3.9	0.1	5.0	0.2	14.9	76.3	39.8	0.6	42.4	22.9	0.8	84.9	114.3
	Med.	1.5	3.7	0.1	5.2	0.2	15.0	64.0	38.0	0.6	40.0	20.0	0.8	53.0	117.0
	S.D.	0.3	1.1	0.0	1.5	0.0	3.1	36.8	14.5	0.1	4.4	7.1	0.0	74.5	21.2
	C.V.	5.1	3.4	5.7	3.2	26.0	4.7	2.1	2.8	11.7	9.6	3.2	33.1	1.1	5.4
	Skew.	−0.1	2.0	1.2	−0.3	0.0	0.7	2.3	0.0	0.4	1.1	1.1	0.2	2.1	1.2
	Kurt.	−0.9	4.4	1.5	−0.8	−1.6	0.2	5.3	−1.3	−0.4	0.2	1.0	−0.7	4.0	2.0
	S-W	0.550	0.002	0.109	0.737	0.004	0.258	0.000	0.445	0.573	0.018	0.102	0.604	0.000	0.079
All	Min.	0.6	1.7	0.0	2.1	0.2	5.0	23.0	7.0	0.5	19.0	5.0	0.7	22.0	39.0
(N = 31)	Max	1.9	10.1	0.1	7.3	0.2	30.0	576.0	63.0	0.8	57.0	61.0	0.9	738.0	270.0
	Mean	1.2	3.9	0.1	4.5	0.2	14.2	91.5	30.2	0.6	39.2	23.7	0.8	104.2	107.8
	Med.	1.2	3.7	0.1	4.6	0.2	14.0	64.0	25.0	0.6	40.0	20.0	0.8	59.0	107.0
	S.D.	0.4	1.6	0.0	1.7	0.0	4.7	96.6	16.8	0.1	8.2	12.9	0.0	131.9	39.1
	C.V.	3.2	2.5	3.6	2.7	23.2	3.0	0.9	1.8	10.2	4.8	1.8	23.0	0.8	2.8
	Skew.	0.2	2.3	1.8	−0.1	−0.6	1.1	4.5	0.5	0.8	−0.3	1.4	1.0	4.0	2.3
	Kurt.	−1.1	7.7	6.5	−1.3	2.0	3.3	22.6	−1.1	0.4	0.4	2.4	1.5	18.6	9.6
	S-W	0.247	0.000	0.001	0.028	0.001	0.029	0.000	0.009	0.110	0.808	0.002	0.056	0.000	0.000
	UCC	15.4	5.0	0.1	4.8	0.1	17.3	92.0	28.0	1.1	47.0	17.0	0.4	97.0	67.0

SD standard deviation, *CV* coefficient of variation, *Skew* skewness, *Kurt* kurtosis, *S-W* Shapiro-Wilk test, *UCC* upper continental crust (Holland and Turekian 2010)

to the deeper southern sectors of the Caspian Sea. Higher contamination levels in the south can also be because of a large number of anthropogenic activities conducted along the southern coasts, including unmanaged emission of contaminants. From a global perspective, the mean concentrations of Cr, Cu, Ni, Pb, and Zn were higher while As and Co were lower in the study area than in most other locations. Similar to most other locations, Cd showed a low concentration of around 0.2 mg kg^{-1}.

Origin of TEs

In general, major anthropogenic activities along the coasts of the southern Caspian Sea comprise farming, fishing, industrial, commercial, touristic, and recreational activities. However, in the west, tourism, farming, and fishing and in the east industrial and commercial activities are more predominant (Fig. 1). Also, the population density in the center and towards the east of the study area is higher than in the west. These anthropogenic activities are considered explanatory factors for the elevated concentrations of some TEs. For instance, Amirabad Special Economic Zone (S13), with 1000 ha of land situated in the east of the region, is an important commercial transit port for oil products and non-oil commercial goods. It is likely that this activity plays an important role in contaminating the surrounding ecosystems.

High levels of Co and Ni may be due to the discharge from agricultural lands and fish farms, containing a variety of chemical fertilizers. Likewise, elevated concentrations of Zn and Cu in the Caspian Sea mainly originate from agriculture return flow containing chemical fertilizers (Bastami et al., 2012). Elevated Cd and Pb content within the samples may

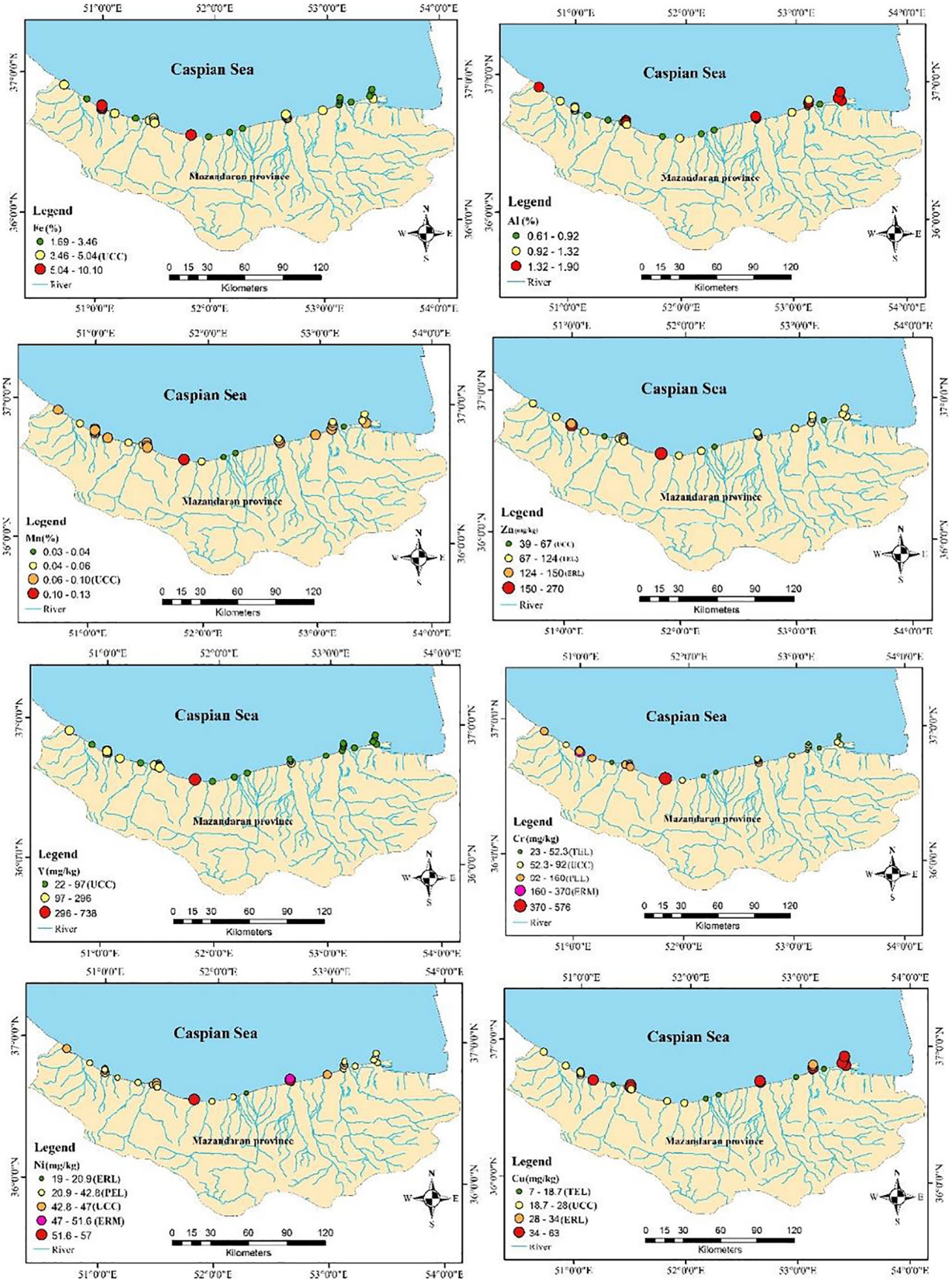

Fig. 3 Spatial distribution of element concentration within coastal and marine sediments, south of Caspian Sea

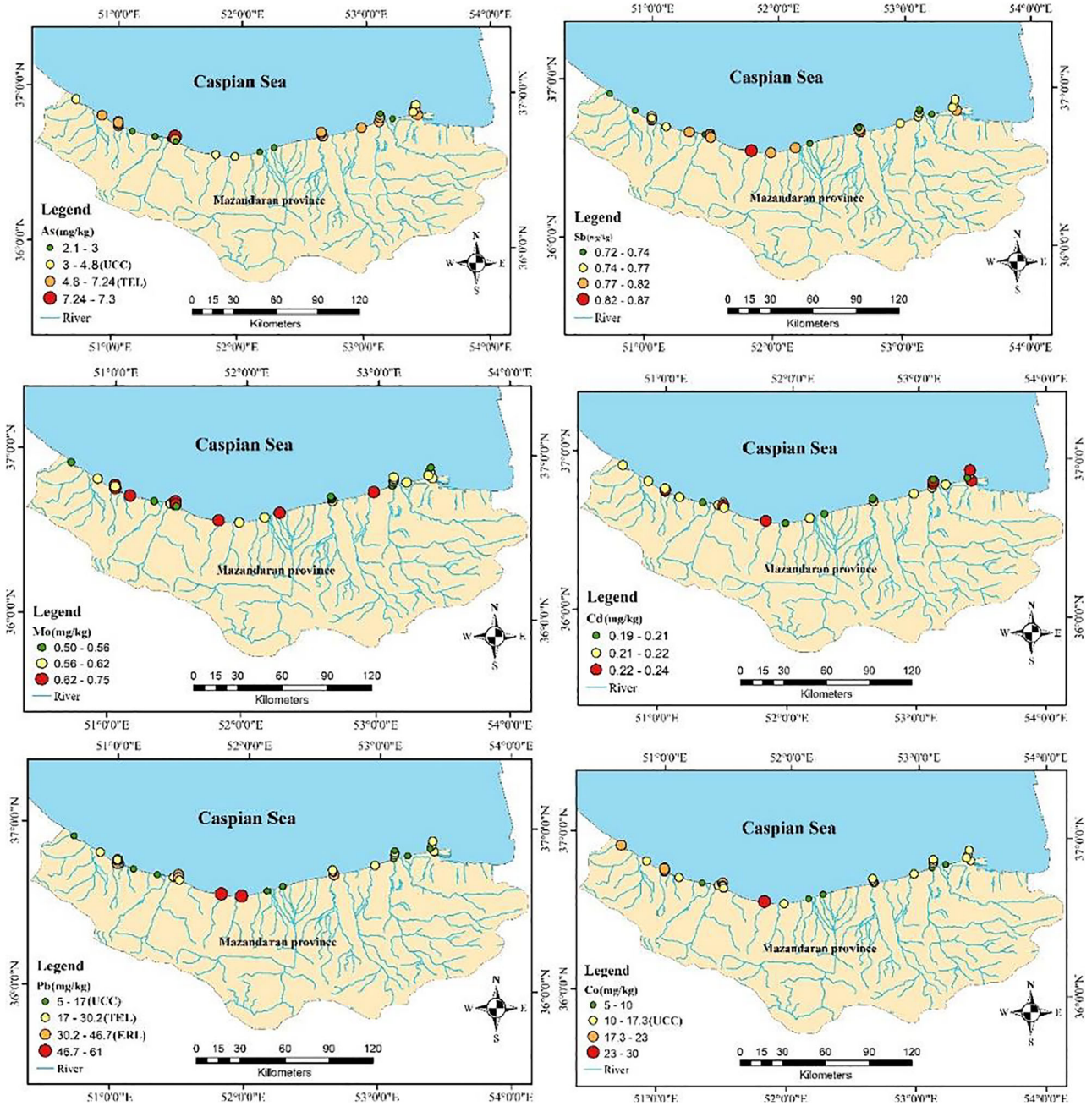

Fig. 3 (continued).

be due to drainages from poorly managed landfilling and from coal layers in the lithological units close to the Caspian Sea (Kalantari and Ebadi, 2006; Ghanbarpour et al., 2013). The large Kura River in the Republic of Azerbaijan, entering the Caspian Sea to the west, is considered a noticeable Cu source into the sea. This runoff is ultimately transferred along the Mazandaran coasts by the prevailing current (De Mora and Turner 2004, Abdi et al. 2009). The major industries in the region are dye and paper manufactures (Tabari et al. 2010, Saravi et al. 2012, Abadi et al. 2019). These industries are responsible for the release of a variety of pigmented TEs such as Pb, Cr, Cd, and Cu into the environment.

Correlation coefficients, presented in Supplementary Material 6, reflected the compositional relationships between elements and sediment physicochemical characteristics. The correlation coefficients indicated no strong positive correlation between sand fraction and TEs, nor any other physicochemical parameters. This shows as expected that shoreline

Table 3 Comparison of mean concentrations (in mg kg^{-1}) of TEs within surface sediments of the study area with those of other locations from the Caspian Sea and worldwide aquatic media

Location	As	Cd	Co	Cr	Cu	Ni	Pb	Zn	Reference
Caspian Sea, Iran	4.5	0.2	14.2	91.5	30.2	39.2	23.7	107.8	This study
Caspian Sea, Iran	NI	NI	16.3	95.0	31.0	53.0	20.0	86.0	Alizadeh et al. (2018)
Caspian Sea, Iran	10.4	NI	30.2	127.4	21.9	47.7	16.0	73.2	Bastami et al. (2015)
Caspian Sea, Iran	NI	1.6	NI	NI	73.1	12.8	24.6	359.9	Naji and Sohrabi (2015)
Caspian Sea, Iran	NI	0.9	NI	NI	14.0	38.6	23.7	51.4	Sohrabi et al. (2010)
Caspian Sea, Iran	12.5	0.2	15.9	85.2	34.7	51.6	18.0	85.3	De Mora et al. (2004)
Caspian Sea, Azerbaijan	14.7	0.1	14.9	85.3	31.9	50.1	19.6	83.2	De Mora et al. (2004)
Caspian Sea, Kazakhstan	4.1	0.1	3.0	31.4	6.4	10.4	5.8	11.1	De Mora et al. (2004)
Caspian Sea, Russia	3.0	0.6	3.8	32.0	8.3	14.0	4.2	17.1	De Mora et al. (2004)
Asaluyeh port, Persian Gulf, Iran	3.7	NI	2.2	16.1	15.4	19.0	3.4	21.1	Delshab et al. (2017)
Changjiang Estuary, China	9.1	0.2	NI	79.1	24.7	31.9	23.8	82.9	Wang et al. (2015)
Central Bohai Sea, China	NI	0.1	13.7	61.5	24.3	35.9	30.7	79.9	Liu et al. (2015)
Intertidal Jiaozhou Bay, China	9.2	0.4	NI	69.9	38.8	NI	55.2	107.4	Xu et al. (2016)
Jiangsu coastal region, China	12.9	0.2	NI	37.2	23.5	NI	16.9	62.2	Zhao et al. (2018)
South Yellow Sea and East China Sea	NI	0.2	NI	77.2	20.0	31.4	21.8	78.4	Xu et al. (2018)
Daya Bay, China	12.4	0.2	NI	65.0	24.6	NI	22.6	111.7	Liu et al. (2018)
Yellow Sea, China	NI	0.51	8.24	NI	15.1	18.6	12.3	47.3	Jiang et al. (2014)
Marine sediments, Point Calimere, India	NI	NI	43.0	59.2	115.5	32.0	NI	738.0	Gopal et al. (2020)
Coromandel beach sediments, India	NI	NI	31.4	344.5	40.6	42.2	68.8	18.8	Gandhi et al. (2020)
Coromandel Coast of India	NI	19.8	51.8	109.5	76.5	28.0	49.6	78.8	Anbuselvan et al. (2018)
Point Calimere, SE coast of India	NI	0.3	51.8	153.0	41.5	54.4	27.5	91.7	Stephen-Pichaimani et al. (2008)
South Sea of Korea	NI	NI	21.0	67.8	27.0	49.0	27.0	131.0	Song et al. (2014)
Egyptian Red Sea coast	NI	0.1	9.7	18.5	1.9	11.4	3.3	22.6	Salem et al. (2014)
Egyptian Mediterranean coast	NI	0.2	NI	NI	11.3	NI	14.8	27.2	El Baz and Khalil (2018)
Saudi Arabian Red Sea coasts	8.3	0.3	6.3	24.8	9.3	14.2	5.6	26.8	Ruiz-Compean et al. (2017)
Coast of Sfax, Gabes Gulf, Tunisia	4.2	8.1	NI	77.2	37.0	11.1	10.7	104.9	Naifar et al. (2018)
Araçá Bay, Brazil	6.5	NI	NI	19.8	5.5	8.1	8.3	36.8	Kim et al. (2018)
Saronikos Gulf, Greece	19.0	NI	9.0	152.0	52.0	77.0	69.0	169.0	Karageorgis et al. (2020)

NI not identified

sediments with sandy texture are not good sinks for TEs. Conversely, the high positive correlations and co-correlations between clay and silt-sized fractions with OM, EC, CEC, and some TEs (e.g., Cu) reflect that seabed sediments are good sinks for TEs as they are bound to the adsorption sites of clay and OM. This is reflected by significant positive co-correlations (r^2 ranging from 0.488 to 0.728) between CEC and As, Co, Cu, Ni, and Zn. Also, the association of TEs with clay and silt fractions (mud) leads to their high co-correlation coefficient with EC, due to the high conductivity in sediments with high CEC.

The significant relationships between TEs and physico-chemical parameters within the sediments were well-understood by the CA model. The dendrogram in Fig. 4 shows how the TEs, as response variables, form clusters with the sediment characteristics, as explanatory variables, depending on their co-variance. Overall, variables form four clusters. The pH, sand fraction, and CO_3 content of the sediments have practically no explanatory value on the TEs. The OM and mud fraction, comprising the silt and clay particle sizes, are inherently clustered with Al due to clay mineral, and CEC and EC due to the large surface area and a number of charged functional groups. These explanatory variables have all a strong explanatory value for the spatial variation in Cu. Practically, all the TEs are clustered with oxyhydroxides of Fe and Mn, although the link to a cluster of As, Ni, and Cd is weak.

The PCA model showed the possible source apportionment of elements, also their meaningful relationships with the sediment characteristics. The Kaiser–Meyer–Olkin factor had a

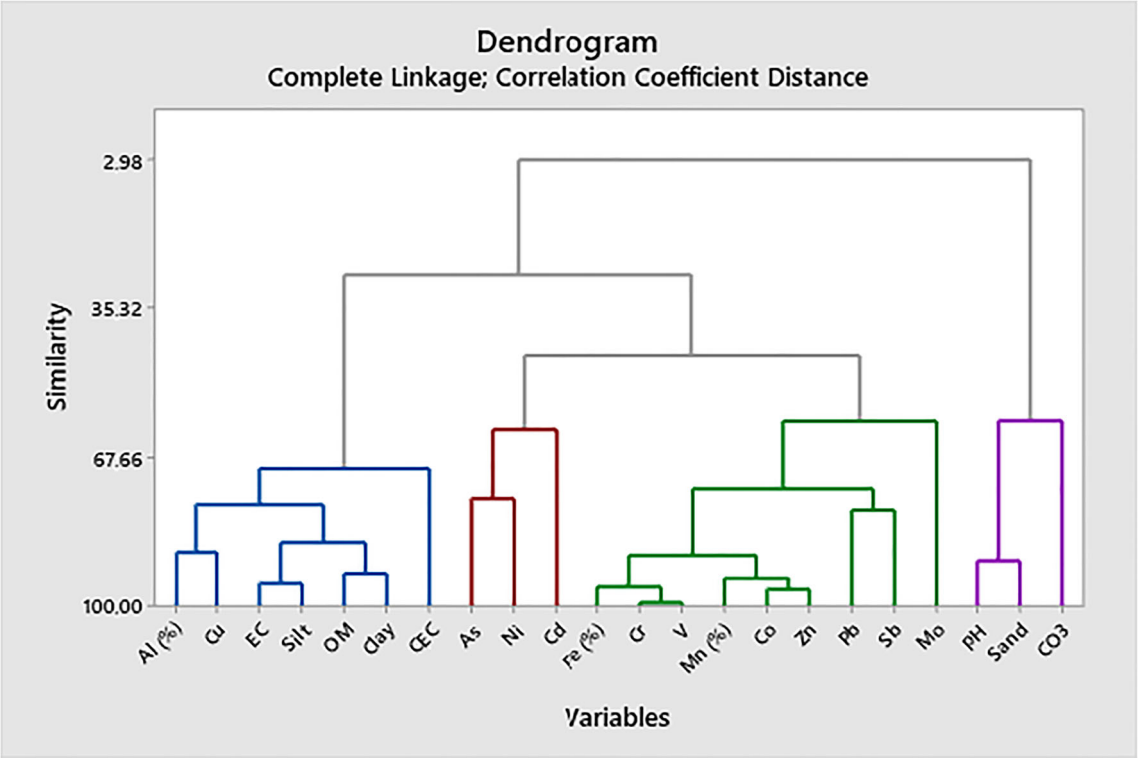

Fig. 4 Dendrogram showing the empirical clustering of explanatory and response variables

value of 0.74. This reflects that the PCA provides significant results for the source apportionment of elements (Wang et al. 2012, Nematollahi et al. 2020b). The PCA gave two major principal components (PC1 and PC2), explaining 35 and 33% of the variance in the dataset, respectively (Fig. 5a). The Fe and Mn have strong loading along the PC1, and the CEC has strong loading along the PC2. The mud size fractions (silt and clay) are along with OM content clustered with EC and Al. This cluster has a significant loading in both PC1 and PC2. Negatively correlated to this cluster along the two main PCs, we find a cluster of sand and pH. The TEs with the strongest loading along PC1 are V, Cr, Zn, and Co. Along PC2, the Cu and Ni have strong loadings. This picture is similar to what was seen in the dendrogram (Fig. 4). The parameter loadings in the PCA separate the effect of Fe and Mn as explanatory factors from the mud and OM content. Sample scores in the PCA (Fig. 5b) show that the shoreline samples had positive and seabed samples had negative scores along the PC2. The least (S7 and S26) and most contaminated samples (S3) had the strongest negative and positive loading along the PC1, respectively. The main epiphanies thus to be received from the PCA are that the spatial distribution in the levels of TEs is governed by the degree of contamination (PC1), possibly governed by the levels of iron oxides in the sediments or by the exposure to anthropogenic pollution sources, and the seashore—seabed gradient (PC2).

Ecological risk of TE

Figure 6a presents the EFs for the TEs. Overall, the results of EF display high enrichment for most TEs, demonstrating a noticeable effect of anthropogenic activity. All TEs have median EFs greater than 5, implying that the sediments are at least moderately polluted. The highest EFs were found for Cd and Sb, with median values above 25, indicating strong to extreme pollution. The median EFs of Zn, Pb, Ni, Cu, and As fall between the reference lines of 10 and 25, reflecting strong pollution. Co, Cr, Fe, Mn, Mo, and V have a median EF value falling between the reference lines of 5 and 10, indicating moderate to strong pollution. The highest individual enrichment factors (EF ≥50) were found for Cr, V, and Zn at site S3, and for Pb at sites S3 and S11.

The CF of TEs is shown in Fig. 6b. Cd and Sb in all samples and Pb and Zn in most of the samples have CFs ranging from 1 to 3. This is suggesting that the sites are only moderately contaminated by these TEs. Moreover, the median CF values of V, Ni, Mo, Cu, Cr, Co, and As are lower than 1, indicating low contamination by these TEs. On the other hand, sites S2 and S3 (Sisangan), site S20, and site S3 are considerably contaminated by Pb, V, and Zn, respectively ($3 < CF \leq 6$). The S3 site shows also very high contamination of Cr and V ($CF \geq 6$). Regarding the CF values, it is possible to conclude that anthropogenic inputs are responsible for the high content of Cd, Sb, Pb, Zn, Cr, and V in the sediment at sites S2 and S3.

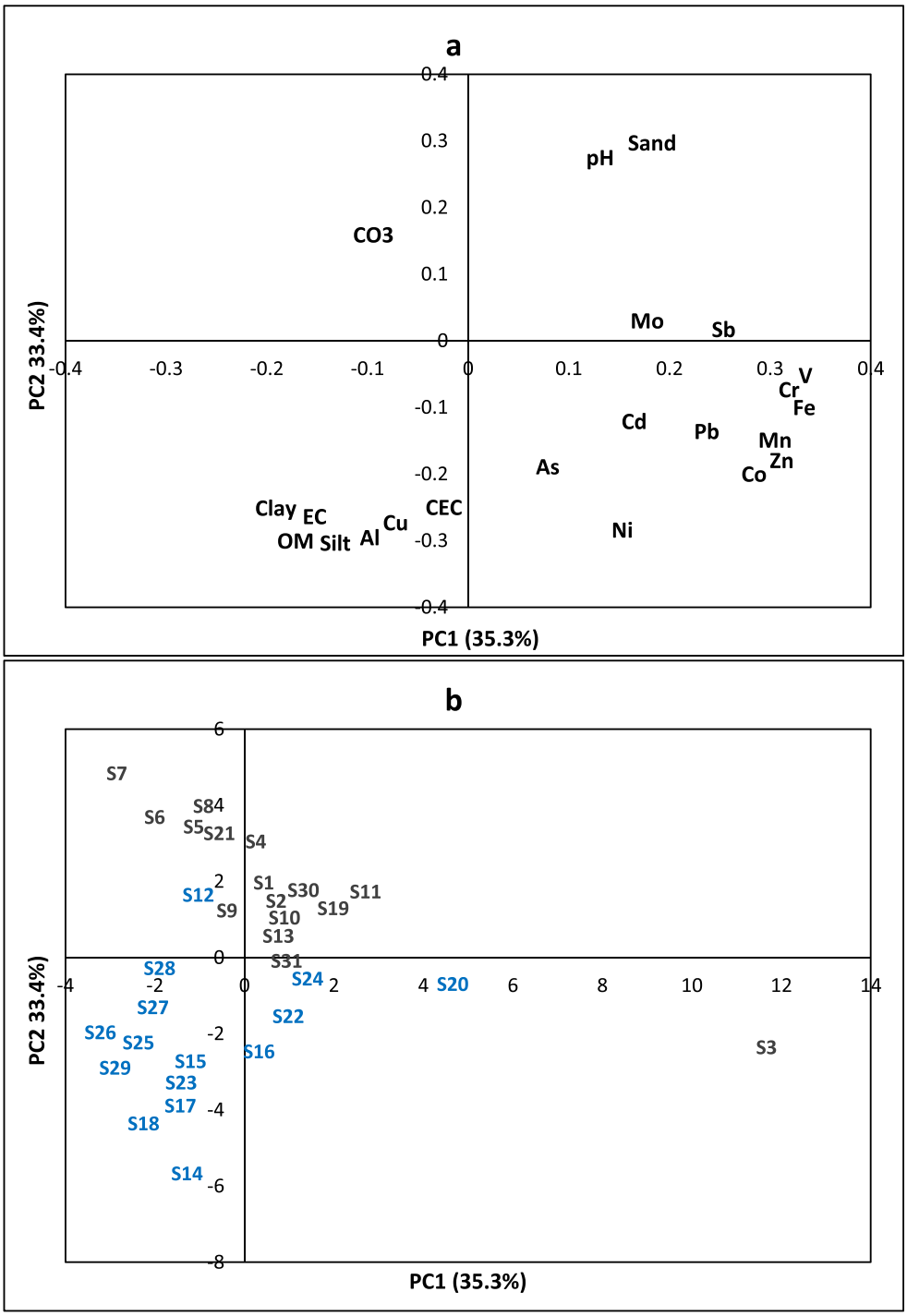

Fig. 5 PCA showing **a** the loadings of explanatory and response variables and **b** the sample scores along the two main principal components, together explaining 68% of the variation in the dataset; seabed samples are shown in blue

The CD indicates very high contamination (CD ≥32) at the S3 site, where also most TEs (e.g., Cd, Sb, Pb, and Zn) were enriched (Fig. 7a). Seven of the 31 sampling sites were considerably contaminated (16 <CD ≤32). The remaining sites had moderate contamination of TEs (8 <CD ≤16).

The integrative multi-element indices assess the general enrichment and the effect of multiple contaminants at a specific site. Overall, the calculated MCD, shown in Fig. 7b, reflects no contamination at most sampling sites (MCD <1.5), although the S3 site with an MCD of 2.51 is moderately polluted (2 <MCD ≤4), and the S20 site with the MCD value of 1.51 is slightly contaminated (1.5 <MCD ≤2). Regarding NPI (Fig. 7c), considering the CFs, only the S3 site is severely polluted (NPI ≥3). However, based on MPI (Fig. 7d), considering the EFs, all sampling sites are characterized as severely polluted (MPI ≥10). Most sites have NPI ranging from 2 to 3, reflecting heavy pollution, while the rest are slightly below reference lines of 2, suggesting moderate contamination.

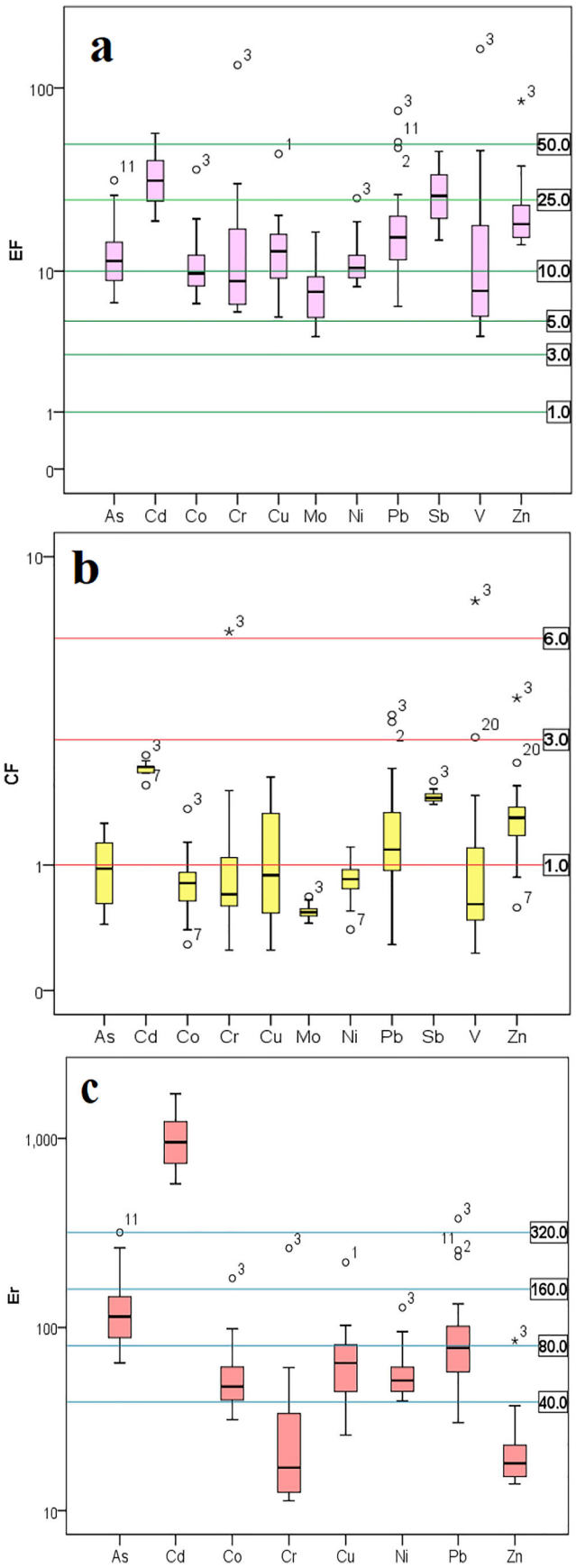

Fig. 6 Ecological risk assessment of elements using **a** EFs, **b** CFs, and **c** Er

Since MPI considers the EFs of TEs, it provides a better assessment of the contamination status by the TEs. Hence, MPI is a good tool to rank the most polluted sites and thus implement optimal abatement actions to decrease the anthropogenic loading at these sites.

The MRI is a multi-element index applied to understand whether a number of toxic elements threaten sediment biota. Based on the calculated Er values for TEs (Fig. 6c), Cd(II) in all sites and Pb(II) at the S3 site show the highest values and pose a very high risk to the ecosystem (Er >320). The risk for ecological detrimental effects is also high in regards to the levels of As(III), Co(II), Cr(VI), Cu(II), and Pb(II) at S11, S3, S3, S1, and S2 and S11, respectively (160 <Er >320). A considerable ecological risk is posed by As(III) in most

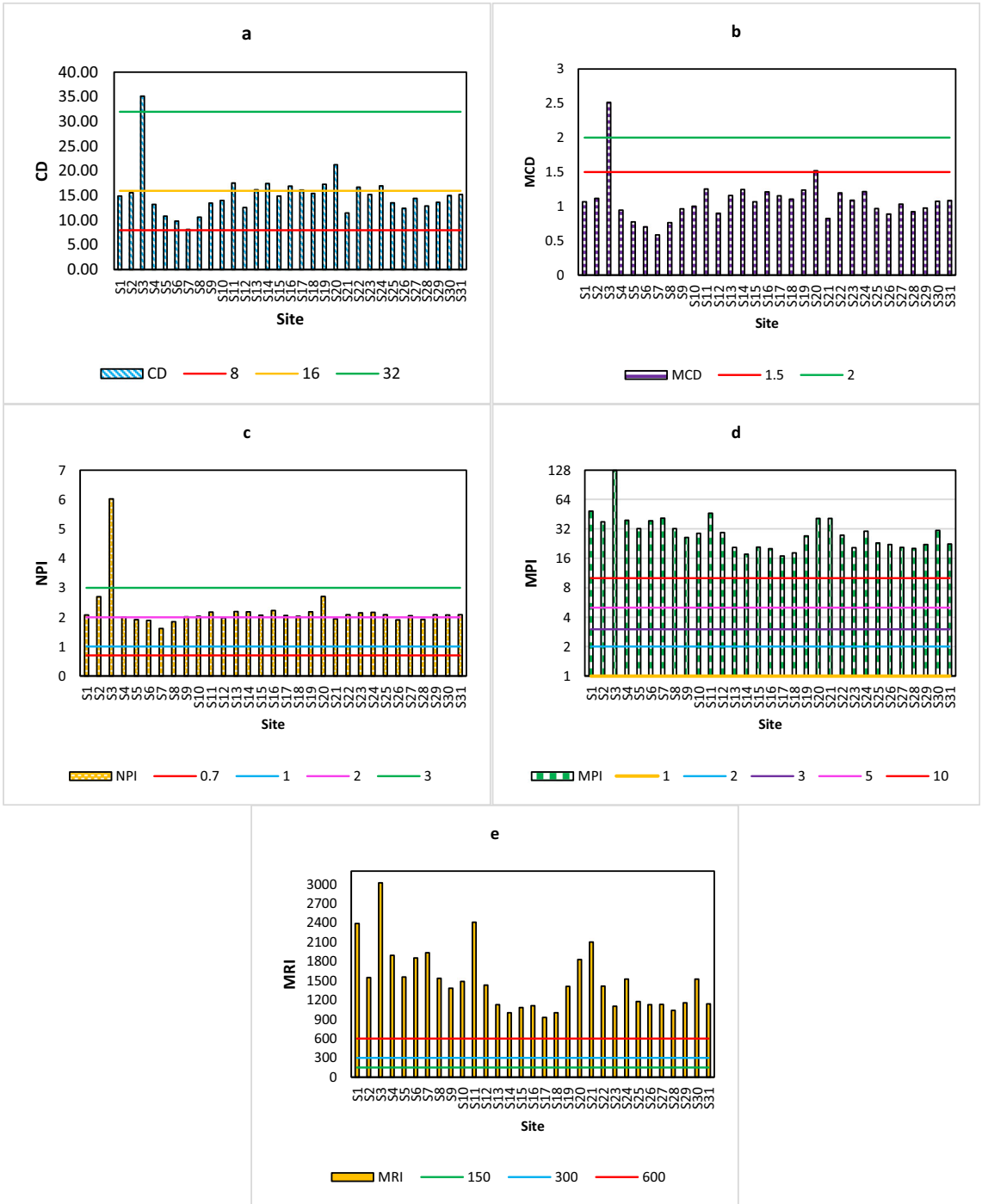

Fig. 7 Ecological risk assessment of sampling sites using **a** CD, **b** MCD, **c** MPI, **d** NPI, and **e** MRI

samples, Pb(II) in some samples, and Ni(II) and Zn(II) at the S3 site. There is a moderate ecological risk due to Co(II), Cu(II), Ni(II), and Pb(II) contamination in most samples (40 <Er <80), while Cr(VI) and Zn(II) pose a low ecological risk in most samples (Er <40). Hence, Cd(II), As(III), and Pb(II) concentrations are a matter of interest as they represent a higher risk to the ecosystem. This is due to the combination of both high toxicity response and enrichment factor of these elements in the sediment. The distribution of the calculated MRI values at each sampling site is illustrated in Fig. 7e. All sampling sites have an MRI value higher than 600. The contamination by toxic TEs thus poses a very high ecological risk in the study area.

Sediment quality

In Supplementary Material 8, the non-normalized and normalized values (relative to the 31 % mud fraction) of SQGs are listed. Considering the non-normalized SQG, the levels of Cr(VI), Cu(II), Pb(II), Ni(II), and Zn(II) were greater than their corresponding ERL values in 10, 10, 2, 30, and 2 sampling sites, respectively. As(III) and Cd(II) had concentrations lower than their ERL values at all sites. The concentrations of Cr(VI) at one site and Ni(II) in two sites were higher than their ERM values, suggesting adverse effects at these sites.

TEL and PEL are indices developed to investigate the unfavorable biological impacts of toxic elements in the aquatic ecosystem. Adverse biological impacts are expected if the concentration of TEs is higher than their PEL values, while they would cause no toxic effect if the TE concentration is lower than their TEL (MacDonald et al. 2000). As(III), Cr(VI), Cu(II), Pb(II), Ni(II), and Zn(II) in S1, S24, S22, S6, S31, and S3 sites displayed concentrations higher than their TEL values, indicating likely negative biological effects to the aquatic biota on the ecosystem. The concentrations of Cr(VI) and Ni(II) in S2 and S8 sites were higher than their PEL values, respectively, suggesting that unfavorable effects of these TEs may occur at a few sites. Considering normalized SQGs, TEs in all sites had concentrations less than their ERL values, though the ERM values were above for Cr(VI) and Ni(II) levels in the majority of sampling stations and Cu and Pb in a limited number of sites. Based on normalized TEL and PEL values, Pb concentration at one site was less than its TEL value, and the levels of Cr(VI), Ni(II), and Cu(II) in S29, S30, and S3 sites were higher than their PEL values.

The m-ERM-Q and m-PEL-Q indices were developed to predict overall toxicity and thereby consider negative ecological effects that occur by exposure to a mixture of elements in sediments (Usman et al. 2013). Based on m-ERM-Q (Fig. 8a), the highest probability of toxicity (46%; 0.51 ≤mERMQ ≤1.5) for the aquatic organisms is at site S3 which should be considered a medium to high priority site. Most sites have an m-ERM-Q value ranging from 0.1 to 0.5, posing a 30% probability for toxicity, which is regarded as low to medium toxicity. The m-PEL-Q value at all sites varies between 0.1 and 1.5 (Fig. 8b), indicating a low to medium toxicity with a toxicity probability of 25%.

Partition coefficient of TEs between water and sediment

The partition coefficient of a substance between aqueous and solid phases indicates its affinity to sorb to the solid (sediment) phase (Anderson and Christensen 1988). Several factors, including the physicochemical characteristics of sediment, the covalent and ionic index of each substance, and the chemical properties of the water, govern the partition coefficient (Allison and Allison 2005, Ahmed and Abdallah 2008).

Adsorption of TEs is largely affected by the distribution of different sorbents such as Al/Fe/Mn oxyhydroxides, clay minerals, and carbonates, as well as OM coating on the sediments. Moreover, the affinity of the TEs to the surfaces is governed by their covalent index. For borderline and class B (soft) metal ions, the pH of the water is usually also considered a key factor in controlling the partitioning coefficient (Kd) (Allison and Allison 2005) as it dictates the precipitation of metal oxyhydroxides as well as the surface charge of the sediments. Moreover, some TEs, such as Sb(V), As(V), and Cr(VI), form oxyanions that will have elevated solubility in the alkaline pH waters found in this study area. The statistical summary of the logarithmic partition coefficients (log Kd) of TEs within the sampling sites is presented in Supplementary Material 9. Pb and Zn have relatively high mean log Kd values (>1), reflecting a strong affinity of these elements to be sorbed and remain in the sediment phase. On the other hand, Cd and Sb are found to have negative mean values for log Kd, reflecting that they prefer to be retained in the aqueous phase. Most soft metals, such as Pb, have low solubility in the natural environment and are retained in the solid phase (Tukura 2015), whereas more soluble elements such as Cd(II) and Sb(V) tend to be more retained in the dissolved state.

There is no significant relationship between the spatial variation in pH and Kd in this research, likely due to the very narrow span in pH (7.83 and 8.55). Although the pH controls the median Kd of some borderline and all class B elements in the study area, this reflects that spatial variation in TE retention on these sediments is largely independent of water pH. The pH is above the point of zero charges for quarts (i.e., net negative charge), in the range for Al and Fe oxyhydroxides, but below for clay minerals and calcite (i.e., net positive charge). The variation in the sediment physicochemical composition, such as mineralogy, carbonate content, and texture, as well as oxyhydroxy and OM coating, suggests heterogeneity of the sediment surface charge and a governing role in determining the spatial variation in Kd values for TEs.

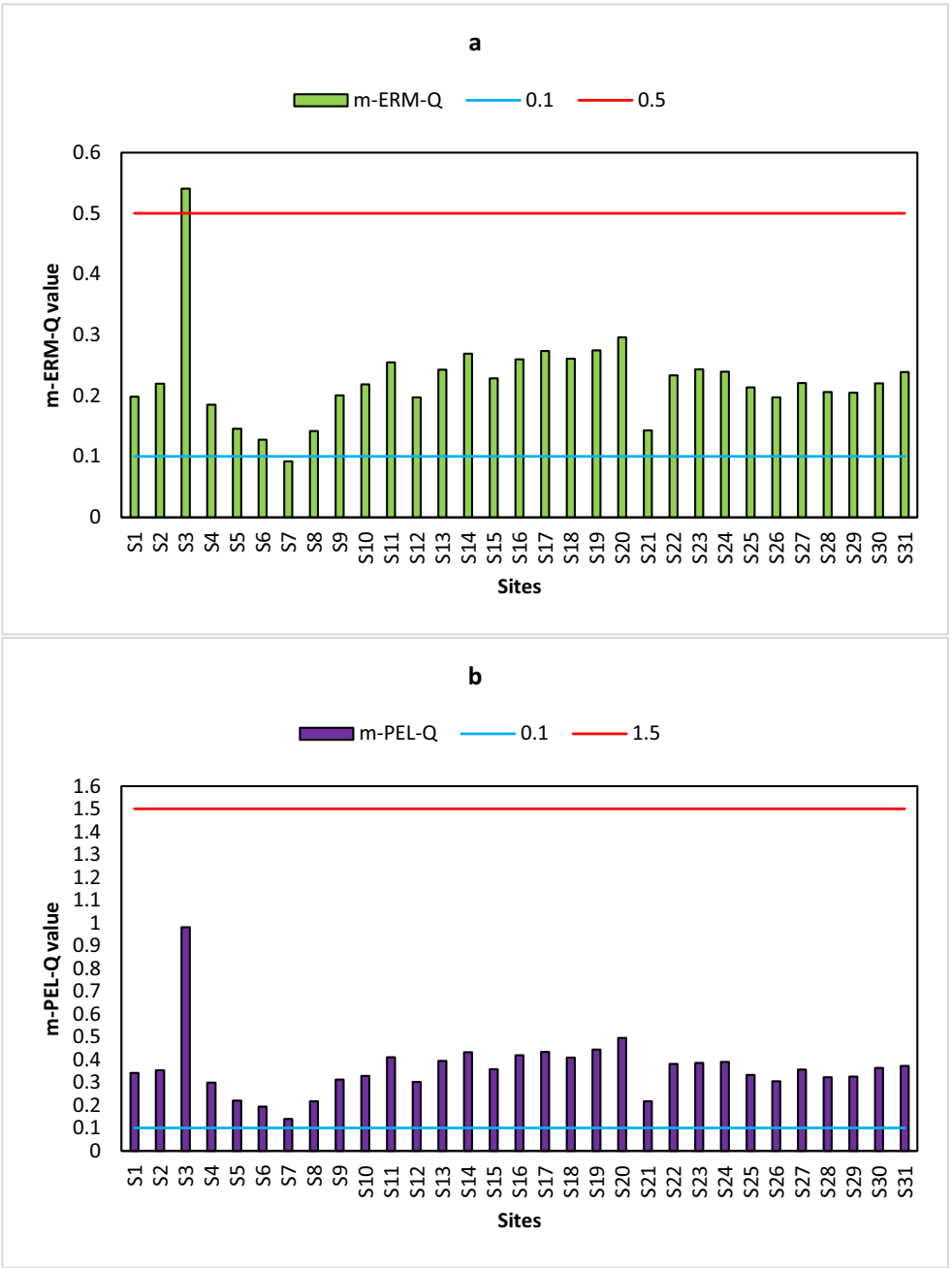

Fig. 8 Values of **a** m-ERM-Q and **b** m-PEL-Q vs. sediment sampling sites

Human health risk of exposure to TEs

To estimate the human health risk of exposure to toxic elements, the ADDs were first computed to determine if the levels of TEs are carcinogenic or not, and their most important exposure pathways to humans (Supplementary Material 10). The health risk was estimated using the computed HQ, HI, CR, and ILCR values (Supplementary Material 11). The median values are presented as these are less influenced by outliers in the non-normal distributed data (Manikandan 2011, Nematollahi and Ebrahimi 2015).

The populations at the investigated sites are mainly exposed to TEs through ingestion. The median ADD_{ing}, ADD_{inh}, and ADD_{derm} values of the non-carcinogenic Zn are the highest among other non-carcinogenic TEs. The median ADD_{ing}, ADD_{inh}, and ADD_{derm} for carcinogenic Cr(VI) (i.e., assuming no Cr(III)) are greatest among other carcinogenic TEs. Based on the HQ, HQ_{ing} has the major contribution, followed by HQ_{derm} and HQ_{inh}. Regarding HI, Cr(VI) has the highest median HI in the subpopulations (adults and children), followed by As(III), Pb(II), Ni(II), Co(II), Cu(II), Zn(II), and Cd(II).

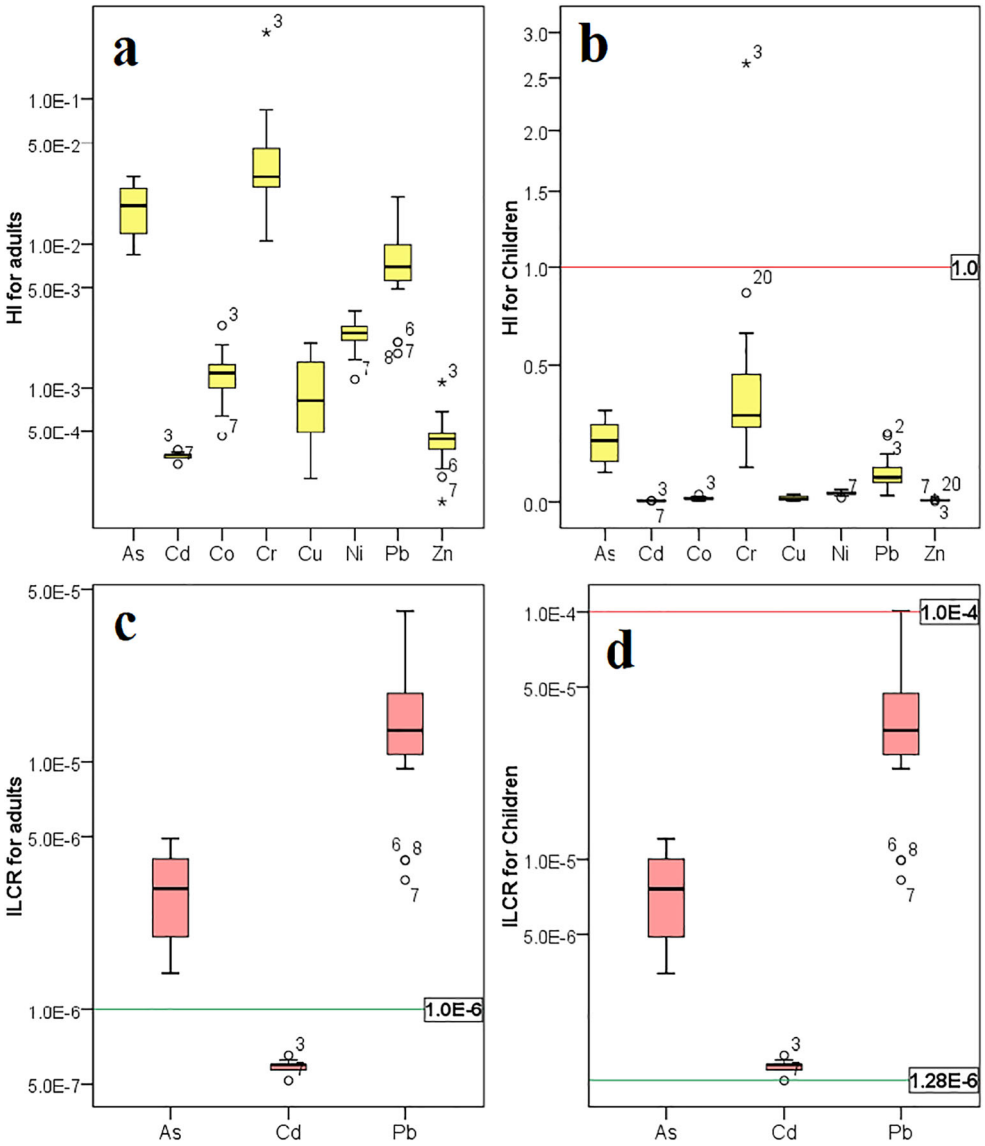

Fig. 9 Box plots showing HI in **a** adults and **b** children, and ILCR in **c** adults and **d** children

As shown in Fig. 9a, TEs have an HI < 1 (the reference value) for adults within the sampling sites, suggesting a minimal non-carcinogenic risk posed on the population at the study sites. However, the HI value of Cr(VI) for children at the S3 site is > 1, posing carcinogenic health risk (Fig. 9b).

Calculated CR indicates that CR_{ing} is the major contributor to ILCR. Local people are therefore mainly exposed to carcinogenic elements through the ingestion pathway. The carcinogenic risk assessment of TEs for the subpopulations, shown in Fig. 9c and d, demonstrates that Pb(II) contributes to the highest carcinogenic risk. Also, Pb(II), As(III), and Cd(II) cause the highest carcinogenic risk (ILCR) for the local people, respectively. Hence, Pb(II) and As(III) at most sampling sites lead to a greater carcinogenic risk for adults than Cd(II). However, Pb(II) and As(III) pose an acceptable or a tolerable risk as their ILCR values range from 10^{-6} to 10^{-4}. Nonetheless, the ILCR value of Cd(II) for adults at all sites is less than 10^{-6}, posing a negligible risk for cancer development. In children, Pb(II), Cd(II), and As(III) have an ILCR value ranging from 10^{-6} to 10^{-4}, constituting a tolerable risk.

Conclusion

Contamination of trace elements (TEs) in shoreline and seabed sediments from the Mazandaran coasts in the south of the Caspian Sea was evaluated in order to gain an improved insight into the levels of their contamination and distribution, as well as possible ecological risk and human health impacts they may be posing. An inhomogeneous and uneven distribution of TEs was observed within both shoreline and seabed sediment sampling stations. This apparently random spatial distribution of the TEs is mainly due to the fact that the study region comprises numerous sources of the TEs from different

potential anthropogenic and natural origins, as well as due to the spatial variation in sediment characteristics. Distinguishing source apportionment of TEs by applying different statistical approaches was thus not feasible. Nevertheless, this study documents that anthropogenic activity in the region discharges TEs to the southern Caspian Sea ecosystem. Fishing industry and shipping are considered two potential in situ sources of TEs, whereas greywater, agriculture, and textile industry introduce TEs from the land into the sea. In addition, leaching from natural weathering of a variety of geological formations in the vicinity of the sea contributes to releasing major and trace elements into the seawater, and their accumulation in shoreline and seabed sediments. Thus, distinguishing different anthropogenic and natural sources of TEs using stable isotopes and rare earth elements in future studies is suggested.

The Sisangan recreational area was identified as the most contaminated site (S3). Geochemical indices indicated higher enrichment of Cd(IV), Sb(V), Zn(II), and Pb(II) at some sampling sites. From a public health perspective, the non-carcinogenic risk of TEs is significant only in the Sisangan area (S3). There is a tolerable carcinogenic risk posed by exposure to Pb(II) and As(III) by adults, and to Pb(II), Cd(VI), and As(III) for children. However, to reach a comprehensive perception of the adverse health effects, bioavailability and speciation of these TEs need to be taken into consideration in future studies.

Supplementary Information The online version contains supplementary material available at https://doi.org/10.1007/s11356-021-14678-9.

Acknowledgements The authors wish to state their gratefulness to Iran's National Elites Foundation (INEF) and Shiraz University Research Committee for logistic supports.

Availability of data and materials All data generated or analyzed during this study are included in this published article (and its supplementary information files).

Author contribution MJN: writing—original draft, conceptualization, methodology, software, formal analysis, investigation, visualization, resources
BK: supervision, resources
FM: supervision, resources
RDV: resources, reviewing, and editing
HNS: supervision

Funding The authors received supports from the X-ray diffraction laboratory of the Department of Chemistry at the University of Oslo, Caspian Sea Ecology Research Center (CSERC), and Medical Geology Research Center of Shiraz University to carry out this research.

Declarations

Ethics approval and consent to participate Not applicable.

Consent for publication Not applicable.

Conflict of interest The authors declare no competing interests.

References

Abadi M, Zamani A, Parizanganeh A, Khosravi Y, Badiee H (2019) Distribution pattern and pollution status by analysis of selected heavy metal amounts in coastal sediments from the southern Caspian Sea. Environ Monit Assess 191(3):144. https://doi.org/10.1007/s10661-019-7261-2

Abdi MR, Hassanzadeh S, Kamali M, Raji HR (2009) 238U, 232Th, 40K and 137Cs activity concentrations along the southern coast of the Caspian Sea, Iran. Mar Pollut Bull 58(5):658–662. https://doi.org/10.1016/j.marpolbul.2009.01.009

Afshin Y (1994) Iran rivers. Ministry of Energy Publication, Tehran, p 1187 [In Persian]

Agah H, Hashtroodi M, Baeyens W (2011) Trace metals analysis in the sediments of the Southern Caspian Sea. J Pers Gulf 2(6):1–12. http://jpg.inio.ac.ir/article-1-43-fa.html

Ahmed M, Abdallah M (2008) Trace metal behavior in Mediterranean-climate Coastal Bay: El-Mex Bay, Egypt and its coastal environment. Global J Environ Res 2:23–29

Alizadeh H, Naderi Beni A, Tavakoli V (2018) Heavy metals in coastal sediments of South Caspian Sea: natural or anthropogenic source? Caspian J Environ Sci 16(1):45–61. https://cjes.guilan.ac.ir/article_2781.html

Allison, J., Allison, T., 2005. Partition coefficients for metals in surface water, soil, and waste. Rep. EPA/600/R-05.

Anbuselvan N, Senthil Nathan D, Sridharan M (2018) Heavy metal assessment in surface sediments off Coromandel Coast of India: implication on marine pollution. Mar Pollut Bull 131:712–726. https://doi.org/10.1016/j.marpolbul.2018.04.074

Anderson PR, Christensen TH (1988) Distribution coefficients of Cd, Co, Ni, and Zn in soils. J Soil Sci 39(1):15–22. https://doi.org/10.1111/j.1365-2389.1988.tb01190.x

Barbosa RN, Overstreet C (2011) What is soil electrical conductivity. LSU AgCenter

Bastami KD, Bagheri H, Haghparast S, Soltani F, Hamzehpoor A, Bastami MD (2012) Geochemical and geo-statistical assessment of selected heavy metals in the surface sediments of the Gorgan Bay, Iran. Mar Pollut Bull 64(12):2877–2884. https://doi.org/10.1016/j.marpolbul.2012.08.015

Bastami KD, Neyestani MR, Shemirani F, Soltani F, Haghparast S, Akbari A (2015) Heavy metal pollution assessment in relation to sediment properties in the coastal sediments of the southern Caspian Sea. Mar Pollut Bull 92(1-2):237–243. https://doi.org/10.1016/j.marpolbul.2014.12.035

Bing H, Wu Y, Zhou J, Sun H, Wang X, Zhu H (2019) Spatial variation of heavy metal contamination in the riparian sediments after two-year flow regulation in the Three Gorges Reservoir, China. Sci Total Environ 649:1004–1016. https://doi.org/10.1016/j.scitotenv.2018.08.401

Bohluly A, Esfahani FS, Namin MM, Chegini F (2018) Evaluation of wind induced currents modeling along the Southern Caspian Sea. Cont Shelf Res 153:50–63.https://doi.org/10.1016/j.csr.2017.12.008

Bouyoucos GJ (1962) Hydrometer method improved for making particle size analyses of soils. J Agron 54(5):464–465

Brady JP, Ayoko GA, Martens WN, Goonetilleke A (2015) Development of a hybrid pollution index for heavy metals in marine and estuarine

sediments. Environ Monit Assess 187:306. https://doi.org/10.1007/s10661-015-4563-x

CEP (2002) Diagnostic Transboundary analysis for the Caspian Sea, vol 2. The Caspian Environment Program, Baku https://ceic-portal.net/index.php/az/node/3060

De Mora S, Sheikholeslami MR, Wyse E, Azemard S, Cassi R (2004) An assessment of metal contamination in coastal sediments of the Caspian Sea. Mar Pollut Bull 48(1-2):61–77. https://doi.org/10.1016/S0025-326X(03)00285-6

De Mora SJ, Turner T (2004) The Caspian Sea: a microcosm for environmental science and international cooperation. Mar Pollut Bull 48: 26–29. https://doi.org/10.1016/S0025-326X(03)00285-6

Delshab H, Farshchi P, Keshavarzi B (2017) Geochemical distribution, fractionation and contamination assessment of heavy metals in marine sediments of the Asaluyeh port, Persian Gulf. Mar Pollut Bull 115(1-2):401–411. https://doi.org/10.1016/j.marpolbul.2016.11.033

Duan CJ, Fang LC, Yang CL, Chen WB, Cui YX, Li SQ (2018) Reveal the response of enzyme activities to heavy metals through in situ zymography. Ecotoxicol Environ Saf 156:106–115. https://doi.org/10.1016/j.ecoenv.2018.03.015

Duodu GO, Goonetilleke A, Ayoko GA (2016) Comparison of pollution indices for the assessment of heavy metal in Brisbane River sediment. Environ Pollut 219:1077–1091. https://doi.org/10.1016/j.envpol.2016.09.008

El Baz SM, Khalil MM (2018) Assessment of trace metals contamination in the coastal sediments of the Egyptian Mediterranean coast. J Afr Earth Sci 143:195–200. https://doi.org/10.1016/j.jafrearsci.2018.03.029

Evans RJ, Davies RJ, Stewart SA (2007) Internal structure and eruptive history of a kilometer scale mud volcano system, South Caspian Sea. Basin Res 19:153–163. https://doi.org/10.1111/j.1365-2117.2007.00315.x

Feng C, Guo X, Yin S, Tian C, Li Y, Shen Z (2017) Heavy metal partitioning of suspended particulate matter–water and sediment–water in the Yangtze estuary. Chemosphere 185:717–725. https://doi.org/10.1016/J.CHEMOSPHERE.2017.07.075

Gandhi KS, Pradhap D, Saravanan P, Krishnakumar S, Kasilingam K, Patel HS et al (2020) Metal concentration and its ecological risk assessment in the beach sediments of Coromandel Coast, Southern India. Mar Pollut Bull 160:111565. https://doi.org/10.1016/j.marpolbul.2020.111565

Ghanbarpour MR, Goorzadi M, Vahabzade G (2013) Spatial variability of heavy metals in surficial sediments: Tajan River Watershed, Iran. Sustain Water Qual Ecol 1:48–58. https://doi.org/10.1016/j.swaqe.2014.04.002

Giralt S, Julia R, Leroy SAG, Gasse F (2003) Cyclic water level oscillations of the Kara Bogaz Gol–Caspian Sea system. Earth Planet Sci Lett 212:225–239. https://doi.org/10.1016/j.swaqe.2014.04.002

Gopal V, Krishnamurthy RR, Kiran DS, Magesh NS, Jayaprakash M (2020) Trace metal contamination in the marine sediments off Point Calimere, Southeast coast of India. Mar Pollut Bull 161: 111764. https://doi.org/10.1016/j.marpolbul.2020.111764

Hakanson L (1980) An ecological risk index for aquatic pollution control. A sedimentological approach. Water Res 14:975–1001. https://doi.org/10.1016/0043-1354(80)90143-8

Heiri O, Lotter AF, Lemcke G (2001) Loss on ignition as a method for estimating organic and carbonate content in sediments: reproducibility and comparability of results. J Paleolimnol 25(1):101–110. https://doi.org/10.1023/A:1008119611481

Holland HD, Turekian KK (eds) (2010) Geochemistry of earth surface systems: a derivative of the treatise on geochemistry. Academic Press

Jiang X, Teng A, Xu W, Liu X (2014) Distribution and pollution assessment of heavy metals in surface sediments in the Yellow Sea. Mar Pollut Bull 83(1):366–375. https://doi.org/10.1016/j.marpolbul.2014.03.020

Kalantari MR, Ebadi AG (2006) Measurement of some heavy metals in sediments from two great rivers (Tajan and Neka) of Iran. J Appl Sci 6:1071–1073. https://scialert.net/abstract/?doi=jas.2006.1071.1073

Karageorgis AP, Botsou F, Kaberi H, Iliakis S (2020) Geochemistry of major and trace elements in surface sediments of the Saronikos Gulf (Greece): assessment of contamination between 1999 and 2018. Sci Total Environ 717:137046. https://doi.org/10.1016/j.scitotenv.2020.137046

Kim BSM, Bícego MC, Taniguchi S, Siegle E, Oliveira R, Alcántara-Carrió J, Figueira RCL (2018) Organic and inorganic contamination in sediments from Araçá Bay, São Sebastião, Brazil. Ocean Coast Manag 164:42–51. https://doi.org/10.1016/j.ocecoaman.2017.12.028

Klige RN, Selivanov AD (1995) Budget of sedimentary material in the Caspian Sea and its possible role in water-level changes. Water Res 22:330–335

Kostianoy AG, Kosarev AN (eds) (2005) The Caspian sea environment, vol 5. Springer Science & Business Media

Lahijani H, Tavakoli V (2012) Identifying provenance of South Caspian coastal sediments using mineral distribution pattern. Quat Int 261: 128–137. https://doi.org/10.1016/j.quaint.2011.04.021

Li T, Sun G, Yang C, Liang K, Ma S, Huang L, Luo W (2019) Source apportionment and source-to-sink transport of major and trace elements in coastal sediments: combining positive matrix factorization and sediment trend analysis. Sci Total Environ 651:344–356. https://doi.org/10.1016/j.scitotenv.2018.09.198

Liu JJ, Ni ZX, Diao ZH, Hu YX, Xu XR (2018) Contamination level, chemical fraction and ecological risk of heavy metals in sediments from Daya Bay, South China Sea. Mar Pollut Bull 128:132–139. https://doi.org/10.1016/j.marpolbul.2018.01.021

Liu M, Zhang A, Liao Y, Chen B, Fan D (2015) The environment quality of heavy metals in sediments from the central Bohai Sea. Mar Pollut Bull 100(1):534–543. https://doi.org/10.1016/j.marpolbul.2015.09.001

Long ER, MacDonald DD (1998) Recommended uses of empirically derived, sediment quality guidelines for marine and estuarine ecosystems. Human Ecologic Risk Assess: Int J 4:1019–1039. https://doi.org/10.1080/10807039891284956

Long ER, Macdonald DD, Smith SL, Calder FD (1995) Incidence of adverse biological effects within ranges of chemical concentrations in marine and estuarine sediments. Environ Manag 19:81–97. https://doi.org/10.1007/BF02472006

Maanan M, Saddik M, Maanan M, Chaibi M, Assobhei O, Zourarah B (2015) Environmental and ecological risk assessment of heavy metals in sediments of Nador lagoon. Morocco Ecol Indic 48:616–626. https://doi.org/10.1016/j.ecolind.2014.09.034

MacDonald DD, Ingersoll CG, Berger TA (2000) Development and evaluation of consensus-based sediment quality guidelines for freshwater ecosystems. Arch Environ Contam Toxicol 39(1):20–31. https://doi.org/10.1007/s002440010075

Manikandan S (2011) Measures of central tendency: the mean. J Pharmacol Pharmacother 2(2):140–142. http://www.jpharmacol.com/text.asp?2011/2/2/140/81920

McCready S, Birch GF, Long ER (2006) Metallic and organic contaminants in sediments of Sydney Harbour, Australia and vicinity-a chemical dataset for evaluating sediment quality guidelines. Environ Int 32:455–465. https://doi.org/10.1016/j.envint.2005.10.006

Menchaca I, Borja Á, Belzunce-Segarra MJ, Franco J, Garmendia JM, Larreta J, Rodríguez JG (2012) An empirical approach to the determination of metal regional sediment quality guidelines, in marine waters, within the European water framework directive. Chem Ecol 28:205–220. https://doi.org/10.1080/02757540.2011.651129

Merhaby D, Ouddane B, Net S, Halwani J (2018) Assessment of trace metals contamination in surficial sediments along Lebanese Coastal Zone. Mar Pollut Bull 133:881–890. https://doi.org/10.1016/j.marpolbul.2018.06.031

Mirnategh SB, Shabanipour N, Sattari M (2018) Seawater, sediment and fish tissue heavy metal assessment in southern coast of Caspian Sea. Int J Pharmaceut Res Allied Sci 7(3):116–125

Moore F, Nematollahi MJ, Keshavarzi B (2015) Heavy metals fractionation in surface sediments of Gowatr bay-Iran. Environ Monit Assess 187(1):4117. https://doi.org/10.1016/j.marpolbul.2018.06.031

Naifar I, Pereira F, Zmemla R, Bouaziz M, Elleuch B, Garcia D (2018) Spatial distribution and contamination assessment of heavy metals in marine sediments of the southern coast of Sfax, Gabes Gulf, Tunisia. Mar Pollut Bull 131:53–62. https://doi.org/10.1016/j.marpolbul.2018.06.031

Naji A, Sohrabi T (2015) Distribution and contamination pattern of heavy metals from surface sediments in the southern part of Caspian Sea, Iran. Chem Speciat Bioavailab 27(1):29–43. https://doi.org/10.1080/09542299.2015.1023089

Nematollahi MJ, Ebrahimi M (2015) Investigation of heavy metals origin in surface sediments of Gowatr Bay, SE Iran using geostatistical analyses. Geochem J 2

Nematollahi MJ, Keshavarzi B, Zaremoaiedi F, Rajabzadeh MA, Moore F (2020c) Ecological-health risk assessment and bioavailability of potentially toxic elements (PTEs) in soil and plant around a copper smelter. Environ Monit Assess 192(10):1–19. https://doi.org/10.1007/s10661-020-08589-4

Nematollahi MJ (2020) Microplastics (MPs) and Potentially Toxic Elements (PTEs) Occurrence in South Caspian Coastal Ecosystem, Mazandaran Province, Ph.D. dissertation. Shiraz University, Shiraz

Nematollahi MJ, Dehdaran S, Moore F, Keshavarzi B (2020b) Potentially toxic elements and polycyclic aromatic hydrocarbons in street dust of Yazd, a central capital city in Iran: contamination level, source identification, and ecological–health risk assessment. Environ Geochem Health 43:485–519. https://doi.org/10.1007/s10653-020-00682-4

Nematollahi MJ, Moore F, Keshavarzi B, Vogt RD, Saravi HN, Busquets R (2020a) Microplastic particles in sediments and waters, south of Caspian Sea: Frequency, distribution, characteristics, and chemical composition. Ecotoxicol Environ Saf 206:111137. https://doi.org/10.1007/s10661-020-08589-4

Pansu M, Gautheyrou J (2007) Handbook of soil analysis: mineralogical, organic and inorganic methods. Springer Science & Business Media

Qingjie G, Jun D, Yunchuan X, Qingfei W, Liqiang Y (2008) Calculating pollution indices by heavy metals in ecological geochemistry assessment and a case study in parks of Beijing. J China Univ Geosci 19:230–241. https://doi.org/10.1016/S1002-0705(08)60042-4

Ribeiro C, Couto C, Ribeiro AR, Maia AS, Santos M, Tiritan ME, Almeida AA (2018) Distribution and environmental assessment of trace elements contamination of water, sediments and flora from Douro River estuary, Portugal. Sci Total Environ 639:1381–1393. https://doi.org/10.1016/j.scitotenv.2018.05.234

Rosado D, Usero J, Morillo J (2016) Assessment of heavy metals bioavailability and toxicity toward Vibrio fischeri in sediment of the Huelva Estuary. Chemosphere 153:10–17. https://doi.org/10.1016/j.chemosphere.2016.03.040

Ruiz-Compean P, Ellis J, Curdia J, Payumo R, Langner U, Jones B, Carvalho S (2017) Baseline evaluation of sediment contamination in the shallow coastal areas of Saudi Arabian Red Sea. Mar Pollut Bull 123(1-2):205–218. https://doi.org/10.1016/j.marpolbul.2017.08.059

Ryan, J., Estefan, G., Rashid, A., 2007. Soil and plant analysis laboratory manual-Google Books.

Salem DMA, Khaled A, El Nemr A, El-Sikaily A (2014) Comprehensive risk assessment of heavy metals in surface sediments along the Egyptian Red Sea coast. Egypt J Aquat Res 40(4):349–362. https://doi.org/10.1016/j.ejar.2014.11.004

Samanta S, Amrutha K, Dalai TK, Kumar S (2017) Heavy metals in the Ganga (Hooghly) river estuary sediment column: evaluation of association, geochemical cycling and anthropogenic enrichment. Environ Earth Sci 76:140. https://doi.org/10.1007/s12665-017-6451-x

Saravi SS, Karami B, Karami S, Shokrzadeh M (2012) Evaluation of metal pollution in fish and water collected from Gorgan coast of the Caspian Sea, Iran. Bull Environ Contam Toxicol 89(2):419–423. https://doi.org/10.1007/s00128-012-0670-3

Singovszka E, Balintova M, Demcak S, Pavlikova P (2017) Metal pollution indices of bottom sediment and surface water affected by acid mine drainage. Metals:7. https://doi.org/10.1007/s00128-012-0670-3

Smith SL, MacDonald DD, Keenleyside KA, Ingersoll CG, Field LJ (1996) A preliminary evaluation of sediment quality assessment values for freshwater ecosystems. J Great Lakes Res 22:624–638. https://doi.org/10.1016/S0380-1330(96)70985-1

Sohrabi T, Ismail A, Nabavi MB (2010) Distribution and normalization of some metals in surface sediments from South Caspian Sea. Bull Environ Contam Toxicol 85(5):502–508. https://doi.org/10.1007/s00128-010-0112-z

Song Y, Choi MS, Lee JY, Jang DJ (2014) Regional background concentrations of heavy metals (Cr, Co, Ni, Cu, Zn, Pb) in coastal sediments of the South Sea of Korea. Sci Total Environ 482:80–91. https://doi.org/10.1016/j.scitotenv.2014.02.068

Stephen-Pichaimani V, Jonathan MP, Srinivasalu S, Rajeshwara-Rao N, Mohan SP (2008) Enrichment of trace metals in surface sediments from the northern part of Point Calimere, SE coast of India. Environ Geol 55(8):1811–1819. https://doi.org/10.1007/s00254-007-1132-9

Sutherland RA (2000) A comparison of geochemical information obtained from two fluvial bed sediment fractions. Environ Geol 39(3-4):330–341. https://doi.org/10.1007/s002540050012

Tabari S, Saravi SSS, Bandany GA, Dehghan A, Shokrzadeh M (2010) Heavy metals (Zn, Pb, Cd and Cr) in fish, water and sediments sampled form Southern Caspian Sea, Iran. Toxicol Ind Health 26(10):649–656. https://doi.org/10.1177/0748233710377777

Thanh-Nho N, Strady E, Nhu-Trang T, David F, Marchand C (2018) Trace metals partitioning between particulate and dissolved phases along a tropical mangrove estuary (can Gio, Vietnam). Chemosphere 196:311–322. https://doi.org/10.1016/J.CHEMOSPHERE.2017.12.189

Tukura B (2015) Heavy metals pollution of water and sediment in Mada River, Nigeria. J Scient Res Rep 6:157–164. https://doi.org/10.9734/JSRR/2015/14803

Turner A (1996) Trace-metal partitioning in estuaries: importance of salinity and particle concentration. Mar Chem 54:27–39. https://doi.org/10.1016/0304-4203(96)00025-4

Tunde OL, Oluwagbenga AP (2020) Assessment of heavy metals contamination and sediment quality in Ondo coastal marine area, Nigeria. J Afr Earth Sci 170:103903. https://doi.org/10.1016/j.jafrearsci.2020.103903

USEPA, 1986. Method 9081: cation-exchange capacity of soils (sodium acetate), part of test methods for evaluating solid waste, physical/chemical methods. https://www.epa.gov/sites/production/files/2015-12/documents/9081.pdf.

USEPA (2011) Exposure factors handbook 2011 edition (Final Report). Washington, D.C: National Center for Environmental Assessment, Office of Research and Development, U.S. Environmental Protection Agency 20460. EPA/600/R-09/052F

Usman AR, Alkredaa RS, Al-Wabel MI (2013) Heavy metal contamination in sediments and mangroves from the coast of Red Sea: Avicennia marina as potential metal bioaccumulator. Ecotoxicol Environ Safety 97:263–270. https://doi.org/10.1016/j.ecoenv.2013.08.009

Violintzis C, Arditsoglou A, Voutsa D (2009) Elemental composition of suspended particulate matter and sediments in the coastal environment of Thermaikos Bay, Greece: delineating the impact of inland waters and wastewaters. J Hazard Mater 166:1250–1260. https://doi.org/10.1016/j.jhazmat.2008.12.046

Voropaev, G.V., 1986. The Caspian Sea: hydrology and hydrochemistry. Nauka, Moscow [In Russian].

Wang H, Wang J, Liu R, Yu W, Shen Z (2015) Spatial variation, environmental risk and biological hazard assessment of heavy metals in surface sediments of the Yangtze River estuary. Mar Pollut Bull 93(1-2):250–258. https://doi.org/10.1016/j.marpolbul.2015.01.026

Wang X, Cai Q, Ye L, Qu X (2012) Evaluation of spatial and temporal variation in stream water quality by multivariate statistical techniques: a case study of the Xiangxi River basin, China. Quat Int 282:137–144.https://doi.org/10.1016/j.quaint.2012.05.015

Xu F, Hu B, Yuan S, Zhao Y, Dou Y, Jiang Z, Yin X (2018) Heavy metals in surface sediments of the continental shelf of the South Yellow Sea and East China Sea: Sources, distribution and contamination. Catena 160:194–200. https://doi.org/10.1016/j.catena.2017.09.022

Xu F, Qiu L, Cao Y, Huang J, Liu Z, Tian X, Li A, Yin X (2016) Trace metals in the surface sediments of the intertidal Jiaozhou Bay, China: sources and contamination assessment. Mar Pollut Bull 104(1-2):371–378. https://doi.org/10.1016/j.marpolbul.2016.01.019

Zhao Y, Xu M, Liu Q, Wang Z, Zhao L, Chen Y (2018) Study of heavy metal pollution, ecological risk and source apportionment in the surface water and sediments of the Jiangsu coastal region, China: a case study of the Sheyang Estuary. Mar Pollut Bull 137:601–609. https://doi.org/10.1016/j.marpolbul.2018.10.044